



## Towards prevention of ischemia-reperfusion kidney injury: Pre-clinical evaluation of 6-chromanol derivatives and the lead compound SUL-138<sup>☆</sup>

PC Vogelaar<sup>a,b,c,#</sup>, D Nakladal<sup>a,d,#</sup>, DH Swart<sup>b</sup>, Ľ Tkáčiková<sup>e</sup>, S Tkáčiková<sup>f</sup>,  
AC van der Graaf<sup>b</sup>, RH Henning<sup>a</sup>, G Krenning<sup>b,c,\*</sup>

<sup>a</sup> Department of Clinical Pharmacy and Pharmacology, University of Groningen, University Medical Center Groningen, Hanzeplein 1, 9713GZ Groningen, Netherlands

<sup>b</sup> Sulfateq B.V., Admiraal de Ruyterlaan 5, 9726GN, Groningen, Netherlands

<sup>c</sup> Cardiovascular Regenerative Medicine, Dept. Pathology and Medical Biology, University of Groningen, University Medical Center Groningen, Hanzeplein 1, 9713GZ Groningen, Netherlands

<sup>d</sup> Department of Pharmacology & Toxicology, Faculty of Pharmacy, Comenius University in Bratislava, Odbojárov 10, 832 32, Bratislava, Slovakia

<sup>e</sup> Department of Microbiology and Immunology, University of Veterinary Medicine and Pharmacy, Komenského 73, 041 81, Košice, Slovakia

<sup>f</sup> Department of Medical and Clinical Biophysics, Faculty of Medicine, Pavol Jozef Šafárik University, Šrobárova 2, 041 80, Košice, Slovakia

### ARTICLE INFO

#### Keywords:

Drug discovery  
Renal failure  
Acute kidney injury  
Pharmacokinetics  
Drug development  
kidney

### ABSTRACT

Acute kidney injury (AKI) is a global healthcare burden attributable to high mortality and staggering costs of dialysis. The underlying causes of AKI include hypothermia and rewarming (H/R), ischemia/reperfusion (I/R), mitochondrial dysfunction and reactive oxygen species production. Inspired by the mechanisms conferring organ protection in hibernating hamster, 6-chromanol derived compounds were developed to address the need of effective prevention and treatment of AKI. Here we report on the pre-clinical screening of 6-chromanol leads that confer protection during I/R to select compounds with favorable profiles for clinical testing in AKI. A library of 6-chromanols ( $n = 63$ ) was screened *in silico* for pharmacochemical properties and druggability. Selected compounds ( $n = 15$ ) were screened for the potency to protect HEK293 cells from H/R cell death and subjected to a panel of *in vitro* safety assays. Based on these parameters, SUL-138 was selected as the lead compound and was found to safeguard kidney function and decrease renal injury after I/R in rats. The compound was without cardiovascular or respiratory effects *in vivo*. SUL-138 pharmacokinetics of control animals (mouse, rat) and those undergoing I/R (rat) was identical, showing a two-phase elimination profile with terminal half-life of about 8 h. Collectively, our phenotype-based screening approach led to the identification of 3 candidates for pre-clinical studies (5%, 3/64). SUL-138 emerged from this small-scale library of 6-chromanols as a novel prophylactic for AKI. The presented efficacy and safety data provide a basis for future development and clinical testing.

**Section assignments:** : Drug discovery and translational medicine, renal, metabolism

**Abbreviations:** AB, Apical to Basolateral; AKI, Acute Kidney Injury; AUClast, Area Under Curve Last; BA, Basolateral to Apical; Caco-2, Colorectal Adenocarcinoma Cells; ClogP, Calculated Partition Coefficient; C<sub>ss</sub>, Concentration at Steady State; E<sub>max</sub>, Maximum Effect; F, Absolute Bioavailability; FDA, Federal Drug Administration; FWHM, Full Width at Half Maximum; H/R, Hypothermia/Rewarming; HEK293, Human Embryonic Kidney Cells; hERG, Human Ether-à-go-go-Related Gene; I/R, Ischemia/Reperfusion; IC<sub>50</sub>, 50% Inhibition Concentration; LC-MS, liquid Chromatography Mass Spectrometry; MAP, Mean Arterial Pressure; NOAEL, No Observed Adverse Effect Level; Papp, Apparent Permeability Coefficient; pEC<sub>50</sub>, log of EC<sub>50</sub>; RAAS, Renin-Angiotensin-Aldosterone System; ROS, Reactive Oxygen Species; S<sub>9</sub>, Fraction of Rat Liver Homogenate; S9f, *Spodoptera frugiperda* cells; SUL, Abbreviation used for new 6-chromanols; t<sub>R</sub>, Retention Time.

<sup>☆</sup>a This work is part of the research program Industrial Doctorates with the project number NWA.ID.17.093 and is partially funded by the Dutch Research Council (NWO). Development of the SUL compound was financially supported by the Northern Netherlands Alliance (SNN) EFRO Tender Valorization. G.K. is supported by Innovational Research Incentive grants from the Netherlands Organization for Health Research and Development (916.11.022 and 917.16.466). D.N. was financially supported by a Abel Tasman PhD scholarship by the Graduate School of Medical Sciences, University of Groningen, University Medical Center Groningen and by Life Sciences and Health - Topconsortium voor Kennis en Innovatie (Stichting LSH-TKI): PPP project-2019-017. b The work presented in this paper has not been published previously in whole or part, not even in abstract form. c Guido Krenning, Sulfateq B.V., Admiraal de Ruyterlaan 5, 9726 GN, Groningen. [g.krenning@sulfateqbv.com](mailto:g.krenning@sulfateqbv.com) Author affiliations: P.C.V. and D.N. contributed equally to this work. Primary laboratory of origin: Department of Clinical Pharmacy and Pharmacology, University of Groningen, University Medical Center Groningen

\* Corresponding author: Dr. Guido Krenning, Sulfateq B.V., Admiraal de Ruyterlaan 5, 9726 GN, Groningen, The Netherlands.

E-mail address: [g.krenning@sulfateqbv.com](mailto:g.krenning@sulfateqbv.com) (G. Krenning).

# Vogelaar and Nakladal contributed equally to this work.

<https://doi.org/10.1016/j.ejps.2021.106033>

Received 28 April 2021; Received in revised form 6 September 2021; Accepted 1 October 2021

Available online 3 October 2021

0928-0987/© 2021 The Authors. Published by Elsevier B.V. This is an open access article under the CC BY license (<http://creativecommons.org/licenses/by/4.0/>).

**Significance statement :** Based on *in silico* druggability parameters, a 63 compound 6-chromanol library was narrowed down to 15 compounds. These compounds were subjected to phenotypical screening of cell survival following hypothermia damage and hit compounds were identified. After subsequent assessment of *in vivo* efficacy, toxicity, pharmacokinetics, and cardiovascular and respiratory safety, SUL-138 emerged as a lead compound that prevented kidney injury after ischemia/reperfusion and demonstrated a favorable pharmacokinetic profile unaffected by renal ischemia.

## 1. Introduction

Acute kidney Injury (AKI) remains a growing global healthcare challenge. The International Society of Nephrology estimates 13.3 million new AKI cases and 1.7 million deaths worldwide each year (International Society of Nephrology. n.d.). In Canada, AKI-related hospital care costs were estimated to increment by \$200 million each year (Collister et al., 2017). In England and the USA, the annual costs of AKI-related hospitalization are estimated at £1.02 billion and \$23.9 billion, respectively (Kerr et al., 2014). Both the patient burden and the staggering costs of AKI treatment are largely attributable to renal replacement therapy, e.g., hemodialysis (Collister et al., 2017). In addition, AKI patients undergoing renal replacement therapy suffer high mortality rates (Levey and James, 2017). Altogether this substantiates a dire need for adequate prevention and pharmacotherapy of AKI.

Strikingly, the incidence of AKI triggered by medical procedures such as cardiac surgery was estimated to 39%, with more than 2 million cardiac surgeries performed worldwide each year (Mehta et al., 2016; Wang and Bellomo, 2017). A major pathophysiological mechanism that underlies AKI in the surgical setting is I/R injury resulting from hypoperfusion, which results from renal vasoconstriction (Wang and Bellomo, 2017). Additional factors that exacerbate renal injury during surgery are hemolysis, inflammation and associated ROS production, non-pulsatile perfusion, adrenergic and/or RAAS activation, and therapeutic or unintentional hypothermia (Wang and Bellomo, 2017). Additionally, extracorporeal circulation can lead to I/R injury, mitochondria-mediated cell damage and death (Wang and Bellomo, 2017). Studies in rodents support the role of mitochondrial dysfunction and the resulting reactive oxygen species (ROS) in the development of AKI (Gao et al., 2015; Morigi et al., 2015). Interestingly, hypothermia and rewarming lead to organ injury and AKI very similar to I/R injury, with most renal impairment occurring during the rewarming period, rather than during hypothermia (Carden and Granger, 2000). Thus, hypothermia/rewarming paradigms may identify targets to prevent or treat AKI in the surgical setting.

Interestingly, small seasonal hibernating mammals alternate between periods with hypometabolism/hypothermia and normal physiology without showing signs of I/R injury (Talaie et al., 2011). Inspired by the underlying protective effects in hibernation (Dugbartey et al., 2014), we developed a set of compounds which have the capability to mimic endogenous mediators involved in hibernation (Salzman et al., 1986; Dugbartey et al., 2015) and ultimately protect kidneys from tubular damage during hypothermia-rewarming (H/R) (Vogelaar et al., 2018). These novel compounds are structural derivatives of 6-chromanol, the core scaffold of tocopherols (vitamin E) (Schmölz, 2016) and Trolox (Scott et al., 1974). Initially, we documented that the 6-chromanol SUL-109 preserves the function of the mitochondrial respiratory chain, thus limiting ROS production during prolonged hypothermia of adipose tissue-derived stromal cells (Hajmoussa et al., 2017). Furthermore, the analogue SUL-121 prevented the progression of albuminuria, vascular endothelial dysfunction, and kidney damage in mice with type 2 diabetes by limiting systemic ROS levels and controlling global redox homeostasis (Lambooy et al., 2017). Finally, we demonstrated that SUL compounds avert kidney injury in rats undergoing deep H/R, by preserving mitochondrial function and limiting DNA damage and protein nitrosylation in renal tubular cells (Vogelaar et al., 2018).

The mentioned compounds are each a racemic mixture of two

enantiomers: SUL-138 contains SUL-132 (*R*) and SUL-138 (*S*), and SUL-121 contains SUL-150 (*R*) and SUL-151 (*S*). Recently, we explored the separate effects of the individual SUL-121 enantiomers in porcine intrarenal arteries and found the (*R*)-enantiomer SUL-150 to antagonize  $\alpha_1$  adrenergic receptors (Nakladal et al., 2019). Based on these previously established protective effects of SUL compounds, we performed a comprehensive pre-clinical characterization of 6-chromanols as the next step in the development of this novel compound class for intravenously administered treatment and/or prevention of AKI in the surgical setting.

## 2. Materials and methods

### 2.1. Pharmacochemical properties

Partition coefficient (ClogP) as a theoretical indicator of hydrophobicity and hydrophilicity, and molecular weight were calculated using Marvin Suite. Even though the objective of the study was to develop a new drug for predominantly intravenous administration, we decided not to limit the use to a single route. Therefore, the Lipinski rule of 5 for oral drugs was used to select a subset of compounds with favorable druggable properties (Lipinski et al., 1997).

### 2.2. Synthesis and formulation

The 6-chromanol library was synthesized by Syncom in Groningen, The Netherlands and was in experimental development before further selecting a subset of compounds. All compounds that were tested *in vitro* (Fig. 1) were dissolved in dimethylsulfoxide (DMSO) with final concentrations lower than 0.5%. Bolus-primed infusions of SUL-138 were administered to rats in 0.9% NaCl/1.67% DMSO. Vehicle controls had equal concentrations of DMSO. Oral administration was done by gavage with compounds or vehicle in corn-oil.

### 2.3. Potency and safety

#### 2.3.1. *In vitro* protection from hypothermia-rewarming

The ability of compounds (50 pM to 100  $\mu$ M,  $n = 6$  per concentration) to preclude hypothermia-induced cell death was assessed using neutral red assay in HEK293 cells cooled at 6 °C. HEK293 cells were seeded on a 96-well plate. After 24 h, culture medium was replaced by pre-warmed cell culture medium containing 6-chromanols (51.2 pM to 100  $\mu$ M,  $n = 6$  per concentration). After 1 h of incubation, cell plates were placed in airtight plastic bags to enclose CO<sub>2</sub> and cultured in the cold room (6 °C for 24 h, followed by rewarming for 2 h under standard culture conditions. Cell viability was measured using Neutral Red Uptake after replacement of the culture medium with 150  $\mu$ L cell culture medium containing 0.4 mg/mL Neutral Red (Sigma-Aldrich, Zwijndrecht, the Netherlands, cat.no. N4638). After an additional 2 h incubation period, Neutral Red solution was aspirated and cell-trapped Neutral Red was solubilized in 100  $\mu$ L solution containing 50% ethanol, 1% acetic acid in dH<sub>2</sub>O. Absorbance was measured at a wavelength of 550 nm in a plate reader (Biotek ELx808, VT, USA). The concentration at which compounds protected 50% of the cells from hypothermia-induced cell death (EC<sub>50</sub> values) were calculated for each compound by performing a 4-parameter logistic curve fit in Graphpad Prism 6.0. The EC<sub>50</sub> values were subsequently converted to pEC<sub>50</sub> by calculating the  $-\log_{10}$  of the EC<sub>50</sub>. The origin and identity of HEK293 cells was confirmed by the

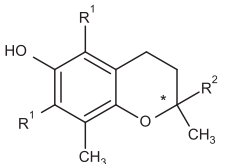
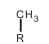
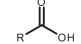
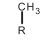
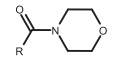
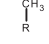
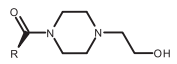
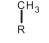
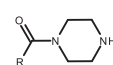
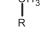
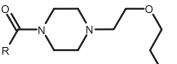
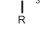
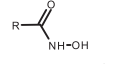
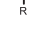
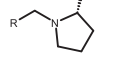
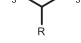
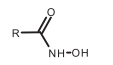

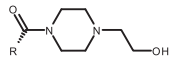
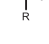
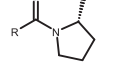
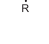
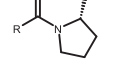
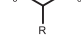
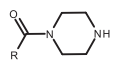
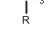
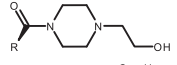
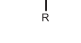
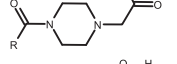
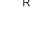
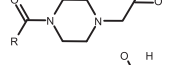

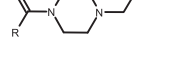

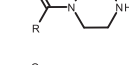
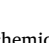
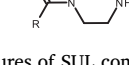
<u>R =</u>			*
<u>name</u>	<u>R<sub>1</sub></u>	<u>R<sub>2</sub></u>	-
Trolox			R/S
SUL-95			R/S
SUL-109			R/S
SUL-121			R/S
SUL-122			R/S
SUL-125			R
SUL-128			S
SUL-131			R/S
SUL-132			R
SUL-134			R
SUL-135			S
SUL-137			R/S
SUL-138			S
SUL-139			R/S
SUL-141			S
SUL-142			R
SUL-150			R
SUL-151			S

Fig. 1. The chemical structures of SUL compounds studied.

supplier (ATCC via LGC Standards S.a.r.l., Molsheim, France).

### 2.3.2. *In vitro* hERG assay

hERG binding was determined with the Predictor™ hERG assay (Thermo Fisher, Blijswijk, the Netherlands) according to the manufacturer's guidelines. 6-chromanols were tested at five concentrations ranging from 0.1 μM to 10 μM. Reference inhibitors included astemizole and E-4031 which were shipped with the kit. Affinity to the hERG receptor was calculated and expressed as IC<sub>50</sub> value.

### 2.3.3. *In vitro* genetic toxicity

Ames mutagenicity (*in vitro* assay) was performed at Eurofins Panlabs (St. Charles, MO, USA) in concurrence to FDA guidelines (Maron and Ames, 1983; Diaz et al., 2007).

### 2.3.4. *In silico* toxicity

Carcinogenicity and *in vitro* mutagenicity were computed in Toxtree v2.6.13 by uploading SMILES structures (Maron and Ames, 1983; Diaz et al., 2007; Kirchmair et al., 2015; R. Benigni et al., 2013; Benigni et al., 2007; Benigni and Bossa, 2011; R. Benigni et al., 2013). The following structures were uploaded: Trolox, Piperazine, 1-(2-hydroxyethyl)-piperazine and the racemic mixtures SUL-109 and SUL-121. Substrates used in the synthesis of SUL compounds, namely Trolox, piperazine and hydroxyethylpiperazine are widely used and well-studied, and were therefore used to calibrate the sensitivity of Toxtree.

## 2.4. *In vitro* pharmacokinetics and disposition

### 2.4.1. Caco-2 passage

As a widely used surrogate tool for human intestinal permeability (Larregieu and Benet, 2013; Artursson, 1990), Caco-2 bidirectional transport was assessed with the MultiScreen Caco-2 assay (Merck, Darmstadt, Germany) using duplicate samples of 10 μM 6-chromanols. Controls included were atenolol and propranolol. The concentrations of 6-chromanols were quantified by LC-MS analysis in each compartment. Apical to basolateral (AB) transport and *vice versa* (BA) were used to calculate the apparent permeability coefficient (P<sub>app</sub>). Efflux ratio was computed by dividing basolateral-apical transport by apical-basolateral (BA/AB).

### 2.4.2. Plasma protein binding

Plasma protein binding (fraction unbound, F%) was performed by spiking duplicate samples of human plasma with 10 μM 6-chromanols and incubating at 37 °C in a Rapid Equilibrium Dialysis (RED) device (Thermo Fisher, Bleiswijk, the Netherlands) according to the manufacturer's guidelines.

### 2.4.3. CYP inhibition assays

CYP inhibition by 10 μM 6-chromanols was tested in triplicate samples using the Vivid® CYP450 kit (Thermo Fisher, Bleiswijk, the Netherlands). For positive control, CYPs 1A2, 3A4, 2C9 and 2D6 were inhibited with α-naphthoflavone, ketoconazole, sulfaphenazole and (+)-quinidine respectively. CYP activity was measured by using a dye that becomes fluorescent once metabolized. Inhibition was calculated using the following formula:

$$\%Inhibition = \left(1 - \frac{X - B}{A - B}\right) * 100\%$$

where X is the enzyme rate of conversion in the presence of 6-chromanols, A is the rate in the absence of 6-chromanol and B is the rate in the presence of the respective positive control.

### 2.4.4. Metabolic stability

Metabolic stability was determined by incubating 6-chromanols (10

$\mu\text{M}$ ) with liver microsomes (1 mg/mL) from various species at 37 °C. Simultaneously, 6-chromanols (10  $\mu\text{M}$ ) were incubated with hepatocytes from various species for 120 min at 37 °C. Samples were taken every 15 min during 1 h and were analyzed by LC-MS.

## 2.5. Chromatography and mass spectrometry

To determine the concentrations of 6-chromanols, blood was first collected in tubes containing EDTA and plasma was obtained by centrifugation at 1800  $\times$  g at 4 °C for 15 min. Proteins in plasma or cell culture medium were then precipitated by adding 2 vol of acetonitrile to each volume of sample, vortexed and incubated for 30 min at -20 °C. The samples were then sonicated for 5 min on ice and centrifuged at 14,000  $\times$  g at 4 °C for 20 min. Supernatant was passed through a 0.22  $\mu\text{m}$  syringe filter and analyzed immediately or stored at -20 °C until further processing.

Liquid chromatography analysis of samples from experiments assessing metabolic stability, Caco-2 permeability, plasma protein binding (F%) and microsomal metabolism was performed on an Acquity HSS T3 column with 1.8  $\mu\text{m}$  pore size 2.1  $\times$  100 mm (Waters, MA, USA). Hepatocyte samples were analyzed on an Acquity Cortecs T3 column with 1.6  $\mu\text{m}$  pore size 2.1  $\times$  50 mm (Waters, MA, USA). Mobile phase A consisted of 0.1% formic acid in water. Mobile phase B consisted of 0.1% formic acid in acetonitrile. The injection volume was 5  $\mu\text{L}$  and chromatography was performed at a flow rate of 0.5 mL/min. Mass spectrometry was performed on a Xevo G2 QToF (Waters, MA, U.S.A.) on Positive Sensitivity Mode MS<sup>E</sup>. Source and desolvation temperatures were 150 °C and 400 °C respectively. Desolvation gas flow was 400 L/h. The capillary was set at 0.5 kV and voltages were 35 V and 4 V for the sampling cone and extraction cone, respectively. Cone gas flow was set to 10 L/h. The resolution was 20,000 (FWHM) and mass range was 200 – 700 Da (hepatocytes) and 200 – 600 (microsomes).

Analysis of 6-chromanol levels in plasma and tissue homogenates was performed using liquid chromatography and mass spectrometry. Plasma or tissue homogenates were mixed with acetonitrile and sonicated, followed by centrifugation at 14,000 g to separate 6-chromanol from the samples and pellet protein precipitates. Tissue samples were subjected to additional solid phase extraction using a SPE Strata C-18 cartridge (100 mg, 55  $\mu\text{m}$ , 70 Å, Phenomenex, Torrance, CA), prepared with 1 ml methanol followed by 1 ml water. Analytes were eluted in acetonitrile:methanol (3%:7% v/v). Analyte recovery was > 70%. Liquid chromatography of the samples was performed on a 1260 Infinity HPLC device (Agilent Tech., Santa Clara, CA) using a ZORBAX Eclipse AAA column (3.0  $\times$  150 mm, particle size 3.5  $\mu\text{m}$ ) in a reversed phase setup and a flow rate of 0.5 mL/min. Solvents consisted of methanol:acetonitrile with 0.1% ammonium acetate (6%/4% v/v) in water and methanol:acetonitrile with 0.1% ammonium acetate (54%/36% v/v) in water for solvent A and B, respectively. MS/MS detection was performed on a QQQ 6460 mass spectrometer (Agilent Tech., Santa Clara, CA). Detection was set for a quantifier ion (205.1, CE 25 V) and qualifier ion (190.1, CE 40 V). Gas temperature for MS was set to 300 °C and flow was set to 6 L/min. Quantification of the samples was performed using an external standard for calibration. LOD and LOQ were 5 and 17 pg/mL, respectively.

## 2.6. In vitro pharmacodynamics

### 2.6.1. Binding and enzyme interaction screen

Radioligand binding assays and enzyme interaction assays were performed by Eurofins Cerep (Celle-Lévescault, France) using a SUL-138 concentration of 10  $\mu\text{M}$ . A total of 71 binding assays and 25 enzyme interactions were studied according to the company protocols.

### 2.6.2. 5-lipoxygenase (5-LO) activity

Activity of the 5-LO enzyme was quantified by measuring the formation of conjugated diene products (5-hydroxyeicosatetraenoic acid,

5-HETE) at 238 nm as previously described (Masferrer et al., 2010). 75  $\mu\text{g}$  of clarified lysate (art.nr. 60,402, Cayman Chemical, MI, USA) from Sf9 cells expressing the human recombinant 5-LO was mixed with dilutions of SUL-138 (1.25, 2.5, 10  $\mu\text{M}$ ) or vehicle in assay buffer (50 mM  $\text{KH}_2\text{PO}_4$ , 300  $\mu\text{M}$   $\text{CaCl}_2$ , 100  $\mu\text{M}$  EDTA, pH 7.2) and incubated at room temperature for 10 min. The enzyme was then added to a solution of 40  $\mu\text{M}$  arachidonic acid (art.nr. 181,198, VWR, Amsterdam, the Netherlands) and 100  $\mu\text{M}$  ATP (art.nr. L14522.03 Thermo Fisher, Karlsruhe, Germany) in assay buffer and absorption at 234 nm was monitored for 5 min at 25 °C. Enzyme activity was determined by calculating the slope of the kinetic curve. For conjugated dienes, an extinction coefficient of 23,000/M/cm was used.

## 2.7. Animal experiments

### 2.7.1. In vivo pharmacokinetics, cardiovascular and respiratory safety

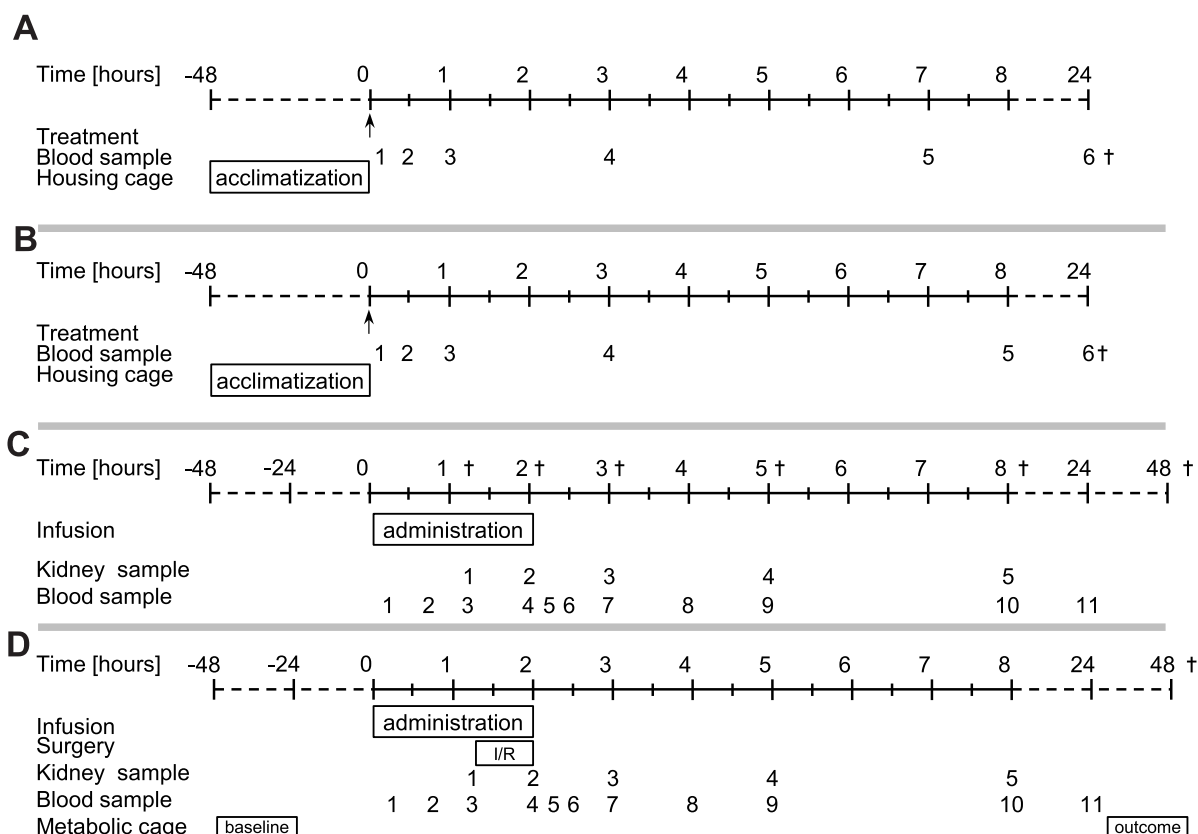
In vivo pharmacokinetic parameters were determined in 1 experiment with mice, and 2 experiments with rats. The mouse experiment, performed at the UMCG (Groningen, the Netherlands), included male 16- to 18-week-old C57BL/6 mice weighing  $28.21 \pm 1.78$  g, that received a permanent jugular vein cannula that was implanted subcutaneously to the head 1 week prior to injection of 6-chromanols (Fig. 2, protocol A). After a blood sample was taken under free moving conditions, mice were administered a single i.v. dose of 10 mg/kg of SUL compound ( $n = 2$ ). Four mice received 30 mg/kg of SUL compounds by oral gavage. Thereafter, blood samples (50  $\mu\text{L}$  in EDTA tubes) were obtained at 0.17, 0.5, 1, 3, 7 and 24 h and compound content was quantified by LC-MS/MS. Food and water were provided *ad libitum* (Fig. 2A).

Subsequent animal studies were performed in rats since these are required by EMA and FDA guidelines for pharmacokinetic studies. In one study performed at the University of Veterinary Medicine and Pharmacy (Košice, Slovakia), male Wistar rats were housed in pairs and received an i.v. injection of 3 mL/kg containing 0.4, 2.0 or 10 mg/kg of SUL compound (Fig. 2B,  $n = 5$  animals per group). Other animals received 10 mL/kg p.o. of 10 mg/kg SUL compound ( $n = 6$ ). Thereafter, blood samples (200  $\mu\text{L}$  in EDTA tubes) were obtained from the tail vein at 0.17, 0.5, 1, 3, 8 and 24 h. Food and water were provided *ad libitum*.

For another study performed by Pharmacology Discovery Services (Taipei, Taiwan), pharmacokinetic parameters were assessed in male Sprague-Dawley rats (Fig. 2C). The animals were anaesthetized with pentobarbital (50 mg/kg i.p.) and were equipped with a carotid artery cannula. SUL-138 was administered by an i.v. bolus (0.1, 0.3 and 0.9 mg/kg), followed by a 2 h continuous infusion (dosing: 0.15, 0.5 and 1.5 mg/kg/h, infusion speed: 1 mL/h). The total administered amounts of SUL-138 were 0.4 mg/kg, 1.3 mg/kg and 3.9 mg/kg. The highest infusion amount was based on the upper limit of solubility. Blood samples (200  $\mu\text{L}$  in EDTA tubes) were collected at 0.25, 0.75, 1.15, 2, 2.25, 2.5, 3, 4, 5, 8, 24 and 48 h. To determine SUL-138 levels in the kidney, animals (2 per timepoint) were euthanized at 1.15, 2, 3, 5, 8 and 48 h after dosing (Fig. 2C). Since 2.5 mg/kg SUL-138 was well tolerated in the 1/R efficacy study, we further escalated the dose to the limit of solubility in 0.5% DMSO. The following dosing regimens were applied: 0.4 mg/kg, 1.3 mg/kg and 3.9 mg/kg.

Cardiovascular and respiratory safety were assessed in male Sprague-Dawley rats. The animals were anaesthetized with pentobarbital (50 mg/kg i.p.) and equipped with a carotid artery cannula connected to a Statham (P23XL) pressure transducer and a NEC/San-Ei Type 366 polygraph (Tokyo, Japan) for direct mean arterial pressure measurements. Heart rate was derived from the pulse pressure recorded on a pen oscillograph (NEC/San-Ei Type 8 K, Tokyo, Japan). Blood samples (0.35 mL) were taken in 10 min intervals and pO<sub>2</sub> levels were immediately analyzed on a blood gas analyzer (Instrumentation Laboratory, MA, USA).

Animal experiments were approved by the Institutional Animal Care and Use Committee of the University of Groningen (CCD 15,167-03),



**Fig. 2.** Animal study protocols. A) C57BL/6 mice ( $n = 2$ ) were administered a single i.v. dose of 10 mg/kg of SUL compound or 30 mg/kg of SUL by oral gavage ( $n = 4$ ). B) Male Wistar rats received an i.v. injection of 3 mL/kg containing 0.4, 2.0 or 10 mg/kg of SUL compound ( $n = 5$ ). In addition, another group of animals ( $n = 6$ ) received 10 mL/kg containing 10 mg/kg p.o. C) Male Sprague-Dawley rats were injected with a single bolus of SUL-138 (0.1 mg/kg, 0.3 mg/kg and 0.9 mg/kg), immediately followed by 2-h intravenous infusion (0.15 mg/kg/h, 0.5 mg/kg/h and 1.5 mg/kg/h). D) Male Sprague-Dawley rats were injected with SUL-138 (0.4 mg/kg, 1.3 mg/kg and 3.9 mg/kg, i.e. upper solubility limit).

the Laboratory of Research Bio-models, Faculty of medicine of the P.J. Šafárik University in Košice (ŠVPS SR - č. k. Ro- 2468/16–221) and the Institutional Animal Care and Use Committee (IACUC) of the Pharmacology Discovery Services Taiwan, Ltd. (575,000–10,162,017). Prior to experiments, animals were housed in type IIIh cages with 2 to 3 animals per cage with a L:D cycle of 12:12 h. Bedding consisted of Asped wood chip (Tapvei, Brogaard, Denmark) and each cage was provided with hiding, nesting and chewing material. Air was exchanged every 5 min. Temperatures were kept at 20 – 24 °C. Diet consisted of Type R36 food (Lantmännen, Kimstad, Sweden) and tap water was provided *ad libitum*. After the experiments, animals were terminated by exsanguination under anesthesia. When applicable, organs were collected and snap frozen for further analysis.

Non-compartmental pharmacokinetic parameters adjusted for animal weights were calculated in R version 3.5.1 (R Core Team 2019) using the package *ncappc* (Acharya et al., 2016). Biphasic concentration profiles of SUL-138 in plasma and kidney were modeled without constraints using the formula:

$$c = dose \times (A^{-a \times (t-1.99)} + B^{-b \times (t-1.99)})$$

where  $c$  is the concentration of drug in plasma or kidney,  $t$  is the time since the administration of bolus-primed infusion,  $A$  and  $B$  are the exponential bases for corresponding compartments, and  $a$  and  $b$  are the slopes of each elimination phase. A single model was fit for each kidney and plasma, and doses (0.4, 1.3 and 3.9 mg/kg) were used as a covariate.

### 2.7.2. In vivo efficacy

Male Wistar rats ( $n = 30$ ) were randomized on weight to sham ( $n = 6$ ) or Ischemia-Reperfusion (I/R,  $n = 24$ ) which was induced by bilateral

renal artery occlusion with vascular clamps for 45 min under anaesthesia (Fig. 2D). Sham animals served as controls for the surgical procedure, and vehicle animals ( $n = 6$ ) underwent I/R and treatment with vehicle (0.9% NaCl/1.67% DMSO). Treated animals ( $n = 6$  per group) received escalating doses of 0.1, 0.5 and 2.5 mg/kg SUL-138 in 0.9% NaCl/1.67% DMSO. Administration occurred through slow i.v. bolus injection 15 min prior to ischemia. After the procedure, animals were housed in a metabolic cage for 24 h to measure food and water intake and to collect urine (Fig. 2D). The study was conducted by Timeline Bioresearch AB (Lund, Sweden) according to Swedish legislation for animal experiments (permit number M154–16). Urine creatinine and electrolytes were determined on a veterinary haematology analyser (Idexx, Kornwestheim, Germany). Urine NGAL (neutrophil gelatinase-associated lipocalin or lipocalin 2), a marker of predominantly tubular cell injury, was analyzed using an ELISA kit (art.nr. ab119602, Abcam, Cambridge, United Kingdom) according to the manufacturer's guidelines. 24 h NGAL levels were calculated by multiplying the NGAL urine concentration (pg/mL) by the 24 h urine volume (mL/24 h).

## 3. Results

### 3.1. Pharmacochemical properties

A pre-existing proprietary library containing 63 synthesized 6-chromanol derivatives was already in experimental development. To advance hits for potential human use, the compounds were screened based on their chemical descriptors including molecular weight, partition coefficients (ClogP), and the Lipinski rule of five for oral drugs (Benet et al., 2016) (Table 1) to determine a subset of candidates for

**Table 1**

Physicochemical properties and *in vitro* potency of SUL compounds. pEC<sub>50</sub> are -log<sub>10</sub> transformed EC<sub>50</sub> values. MW, molecular weight; TPSA, total polar surface area; ClogP, calculated partition coefficient.

ID	MW	TPSA	ClogP	HEK293 pEC <sub>50</sub> [-log <sub>10</sub> (M)]
Trolox	250.29	66.76	3.01	4.42
SUL-95	319.40	59.00	2.84	7.50
SUL-109	362.46	73.24	2.25	7.87
<b>SUL-121</b>	<b>318.40</b>	<b>61.80</b>	<b>2.60</b>	<b>8.56</b>
SUL-122	406.52	82.47	1.56	7.90
SUL-125	265.30	78.79	2.91	6.84
SUL-128	319.44	52.93	4.06	7.74
SUL-131	321.42	82.47	3.88	7.64
SUL-132	362.46	73.24	1.84	8.40
SUL-134	333.42	70.00	3.05	7.94
SUL-135	333.42	70.00	3.05	7.80
SUL-137	374.53	61.80	3.57	7.67
<b>SUL-138</b>	<b>362.46</b>	<b>73.24</b>	<b>1.84</b>	<b>8.60</b>
SUL-139	432.55	90.31	1.01	6.99
SUL-141	376.46	90.31	0.04	6.21
SUL-142	376.46	90.31	0.04	7.43

further *in vitro* profiling. All compounds complied with the molecular weight criterion lower than 500 g/mol, with the heaviest being 432.55 g/mol (SUL-139). 6-chromanols with ClogP higher than 5 were excluded. None of the derivatives contained more than 3 hydrogen bond donor groups and the highest number of hydrogen bond acceptors in a single molecule was 7 (SUL-104, SUL-105, SUL-122, SUL-136, SUL-139, SUL-140, SUL-141, SUL-142), thus complying with Lipinski's criteria for hydrogen bonds (Benet et al., 2016). By applying the above criteria on the initial set of 63 compounds, compounds were excluded based on exceeding theoretical ClogP, resulting in a subset of 15 candidates selected for further screening.

**Table 2**

Pharmacokinetic properties of SUL compounds. Intestinal absorption represented by Caco-2 permeability, plasma protein binding by fraction of compound unbound, liver Cytochrome P450 enzyme inhibition and metabolic stability in human and rat microsomes measured at 10 μM concentration. P<sub>app</sub>, apparent permeability coefficient; AB, apical to basolateral transport; BA, basolateral to apical transport; ∞, infinitely long (negative calculated t<sub>1/2</sub>). Grey cell shading represents values meeting exclusion criteria.

ID	Caco-2 cell permeability		Efflux ratio	Fraction unbound [%]	Human liver enzyme inhibition [%]				Metabolism			
	P <sub>app</sub> (AB) [10 <sup>-5</sup> cm/s]	P <sub>app</sub> (BA) [10 <sup>-5</sup> cm/s]			CYP1A2	CYP2C9	CYP2D6	CYP3A4	human microsomes [%] at 30 min	t <sub>1/2</sub> [h]	rat microsomes [%] at 30 min	t <sub>1/2</sub> [h]
Trolox	4.46	4.04	0.91	12.0	0.0	-2.0	-9.0	15.0	99.5	19.25	93.4	5.10
SUL-95	4.26	3.14	0.74	20.0	21.0	40.0	-10.0	43.0	69.0	1.00	14.0	0.23
<b>SUL-121</b>	<b>1.93</b>	<b>3.38</b>	<b>1.75</b>	<b>37.0</b>	<b>14.0</b>	<b>2.0</b>	<b>-1.0</b>	<b>18.0</b>	<b>86.0</b>	<b>4.60</b>	<b>79.0</b>	<b>1.67</b>
SUL-122	1.14	2.98	2.61	41.0	-4.0	-2.0	-9.0	6.0	86.0	1.55	75.0	1.02
SUL-125	3.87	2.50	0.65	25.0	8.0	4.0	0.0	9.0	95.0	5.98	73.0	1.08
SUL-128	3.90	2.39	0.61	9.0	19.0	4.0	74.0	32.0	88.0	4.35	13.0	0.22
SUL-131	3.60	2.12	0.59	12.0	21.0	38.0	-9.0	13.0	84.0	2.33	45.0	0.45
SUL-132	2.24	2.83	1.26	45.0	-1.0	-5.0	-2.0	3.0	70.0	1.38	70.0	1.20
SUL-134	3.21	3.09	0.96	19.0	10.0	24.0	-4.0	41.0	47.0	0.68	29.0	0.27
SUL-135	2.50	2.79	1.12	13.0	13.0	11.0	-2.0	10.0	67.0	1.82	26.0	0.28
SUL-137	2.93	3.13	1.07	10.0	36.0	25.0	0.0	69.0	68.0	1.67	66.0	0.78
<b>SUL-138</b>	<b>2.36</b>	<b>3.01</b>	<b>1.28</b>	<b>31.0</b>	<b>5.0</b>	<b>1.0</b>	<b>5.0</b>	<b>17.0</b>	<b>77.0</b>	<b>5.38</b>	<b>83.0</b>	<b>2.17</b>
SUL-139	7.42	1.33	0.18	25.0	4.0	18.0	2.0	35.0	91.0	∞	114.0	∞
SUL-141	9.22	1.51	0.16	56.0	1.0	2.0	0.0	4.0	86.0	∞	106.0	2.13
SUL-142	1.23	1.46	1.19	72.0	-1.0	4.0	0.0	0.0	82.0	∞	110.0	∞

### 3.2. *In vitro* potency

Selected 6-chromanols were screened for their potency in protecting human embryonic kidney cells (HEK293) from hypothermia-induced cell death. All 15 compounds effectively inhibited hypothermia-induced cell death with an efficacy (E<sub>max</sub>) reaching 100% survival. The least potent compound was Trolox with EC<sub>50</sub> = 38 μM, while the compounds SUL-121 (EC<sub>50</sub> = 2.7 nM) and SUL-138 (EC<sub>50</sub> = 2.5 nM) demonstrated far more advantageous protection of cells from hypothermia (Table 1). The two most potent compounds SUL-121 and SUL-138 were preferred over SUL-122 (EC<sub>50</sub> = 12.59 nM) and SUL-125 (EC<sub>50</sub> = 144.54 nM) mainly on the basis of *in vitro* efficacy in protecting HEK293 cells from H/R-induced death. Also, when considering the R<sub>2</sub> substituent on SUL-122, it contains a 6-atom tail chain that carries rotatable bonds which result in high flexibility that could reduce bioavailability (Veber et al., 2002). In contrast, SUL-121 (no tail chain) and SUL-138 (3-atom tail chain) are considerably less flexible. The compound SUL-125 contains a hydroxamide substituent on R<sub>2</sub> that more closely resembles Trolox than the compounds SUL-121 and SUL-138, which contain the larger piperazinecarboxamide group.

### 3.3. *In vitro* disposition

We assessed bidirectional Caco-2 cell permeability of the 15 SUL compounds as a representation of human intestinal absorption and efflux (Table 2). The reference compounds atenolol and propranolol were used to verify the assay. Propranolol falls into the high permeability drug category due to passive transcellular transport (P<sub>app</sub> > 1.0 × 10<sup>-5</sup> cm/s) and atenolol is expected to have a lack of permeability with P<sub>app</sub> < 1.0 × 10<sup>-5</sup> cm/s. Indeed, atenolol was (P<sub>app;A>B</sub> = <LLOQ and P<sub>app;B>A</sub> = 2.78 × 10<sup>-5</sup> cm/s) being less permeable than propranolol (P<sub>app;A>B</sub> = 3.96 × 10<sup>-5</sup> cm/s and P<sub>app;B>A</sub> = 2.42 × 10<sup>-5</sup> cm/s). The

$P_{app,B>A/A>B}$  ratios were 0.61 for propranolol, and unavailable for atenolol due to absent  $P_{app,A>B}$ . The subset of 6-chromanols generally demonstrated high apical-basolateral permeability (Zheng and Yang, 2008; van Breemen and Li, 2005; Takano et al., 1998), as reflected by their  $P_{app}$  ranging from 1.14 to  $9.22 \times 10^{-5}$  cm/s for SUL-122 and SUL-141, respectively (Table 2). In contrast, efflux ratios of SUL compounds were lower than 2 across the compound library, with the exception of SUL-122 (efflux ratio: 2.61), suggesting that SUL compounds are not subjected to active flux to the intestine (Table 2) (Cyprotex, n.d.). SUL-121 and SUL-138 passed our cutoff criterion with efflux ratios 1.75 and 1.28 respectively (Table 2).

Protein binding was assessed in pooled human plasma, and expectedly correlated with lipid solubility (Fig. 3A). Compounds were classified based on recommendations of the European Bioanalysis Forum (Buscher et al., 2014). The 6-chromanols Trolox, SUL-128, SUL-131, SUL-135 and SUL-137 had an unbound fraction below 15% and therefore were flagged as high protein binders and discarded from further development (Table 2). Despite many registered drugs having this property, we opted for the benefits of higher tissue penetration and shorter terminal half-lives of low-protein binders. SUL-121 and SUL-138 were classified as medium to low plasma protein binders with their unbound fractions amounting 37% and 31% respectively (Table 2, Fig. 3A).

Next, we measured liver cytochrome P450 (CYP) inhibition by SUL compounds to explore risk of drugs interactions. At 10  $\mu$ M concentrations, SUL-121 and SUL-138 passed our criterion of maximum 20% inhibition of tested CYP enzymes (Table 2). SUL-137 inhibited CYP1A2 by 36% and was therefore excluded from further studies. SUL-95 and SUL-131 were the strongest inhibitors of CYP2C9, while SUL-128 strongly inhibited CYP2D6 and SUL-137 CYP3A4 (Table 2).

### 3.4. Metabolism

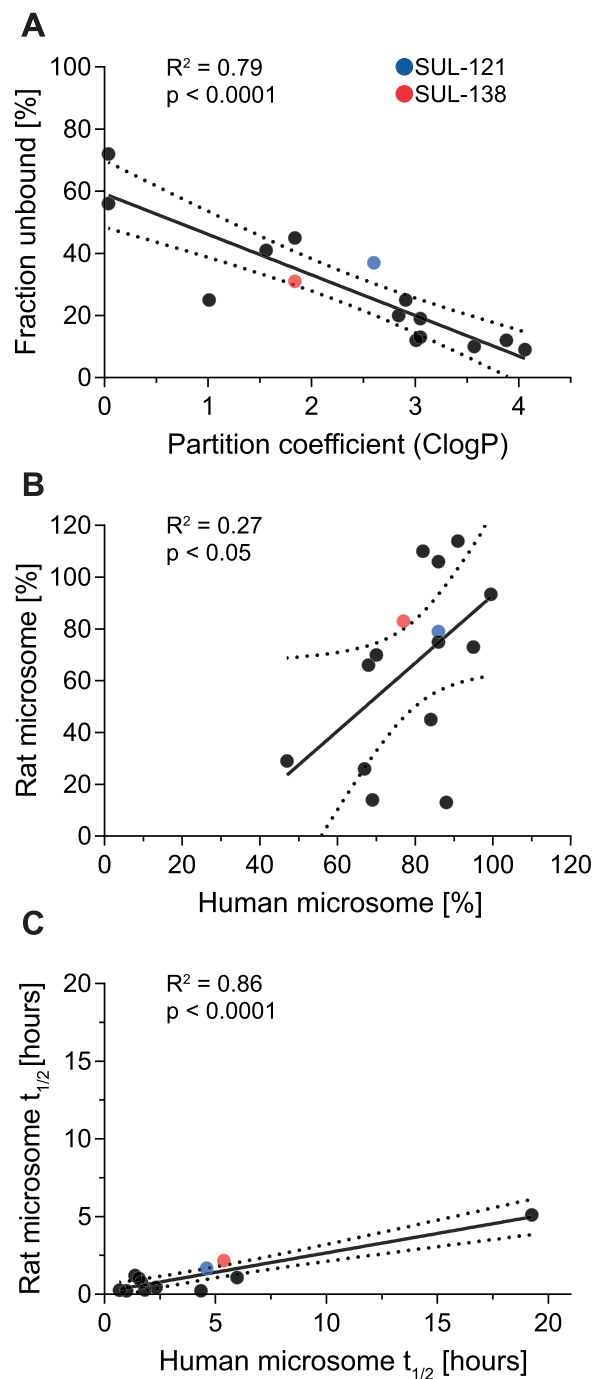
#### 3.4.1. Metabolic degradation

Metabolism of SUL compounds was assessed as the amount of unchanged compound after 30 min of incubation with human or rat liver microsomes. Trolox (99.5% human, 93.4% rat microsomes) and SUL-125 (95% human microsomes) were minimally metabolized, and high fractions of SUL-139 and SUL-141 were recovered in both species of microsomes, also indicative of low metabolism (Table 2). On the other end of the spectrum, SUL-134 was found in less than half of its original concentration after 30 min exposure to human (47%) and rat (29%) microsomes (Table 2). The metabolism of SUL-121 and SUL-138 was comparable between human and rat microsomes and was considered moderate within the range of our subset of 6-chromanols (Table 2, Fig. 3B). Additionally, the *in vitro* metabolism was estimated by determining half-life ( $t_{1/2}$ ) using 15 min sampling intervals during 60 min incubation with human and rat liver microsomes. The terminal half-lives of SUL-121 and SUL-138 in human microsomes were in a similar range amounting 4.6 h and 5.4 h, respectively. Given the described properties, the compounds SUL-121 and SUL-138 were considered most suitable for further development (Table 2, Fig. 3C).

#### 3.4.2. Metabolites

Considering the racemic character of SUL-121 and our recent discovery of the  $\alpha$ -adrenoceptor antagonistic property of its (*R*)-enantiomer (Nakladal et al., 2019), we decided to further develop and investigate SUL-138. This decision was further supported by the fact that SUL-138 shares the chiral (*S*)-configuration with SUL-151 that lacks vascular effects (Nakladal et al., 2019).

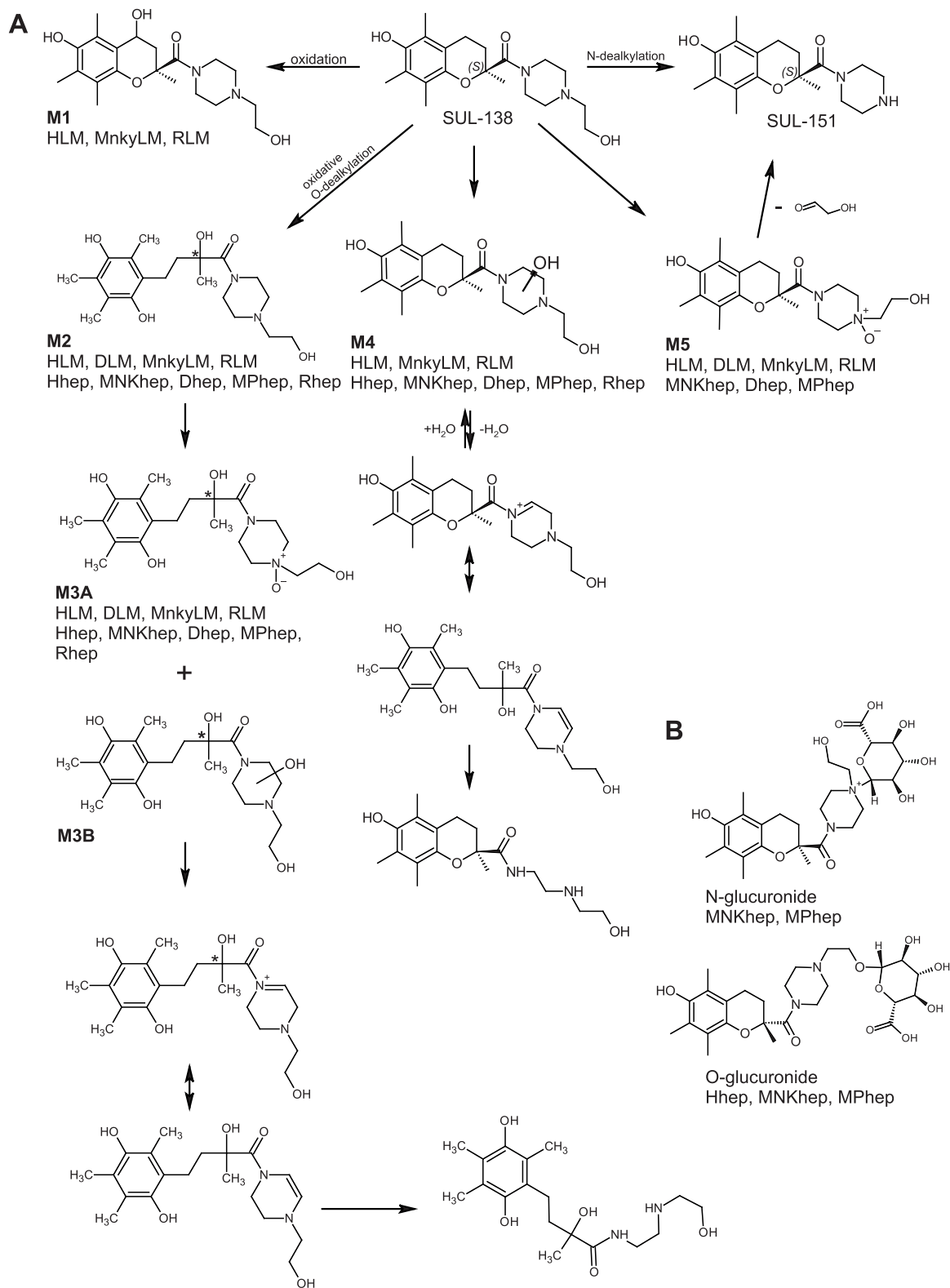
The individual metabolites of SUL-138 (10  $\mu$ M) were further studied qualitatively and quantitatively in human, Cynomolgus monkey, Beagle dog and Sprague-Dawley rat liver microsomes and hepatocytes, and in hepatocytes of Gottingen minipig by full scan LC-MS/MS analysis. Five phase I metabolites and 2 phase II conjugates were identified, and their corresponding peak areas and retention times (tR) recorded (Fig. 4).



**Fig. 3.** Correlations between *in vitro* parameters of 6-chromanols. A) Relationship between theoretical solubility represented by predicted water/octanol partition coefficient ClogP and human plasma protein binding of SUL compound, B) Metabolic stability of 6-chromanols after 30 min incubation with human and rat liver microsomes expressed as % compound remaining, and C) half-lives of 6-chromanols in human and rat liver microsomes.

#### 3.4.3. Human

The first eluting metabolite, M1 (tR = 3.19 min) was formed by the oxidation of C4 of the chromanol moiety and was detected in human microsomes but not detected in hepatocytes (Fig. 4A, Fig. 5). The main human microsome and hepatocyte metabolite M2 (tR = 3.38 min) was a product of oxidative O-dealkylation on C1 of the heterocyclic chromane, which led to the opening of the chromane scaffold, effectively forming a quinol (Fig. 4A, Fig. 5). Such reaction is known to be important in the metabolism of tocopherols (vitamin E) (Schmölz, 2016). Further

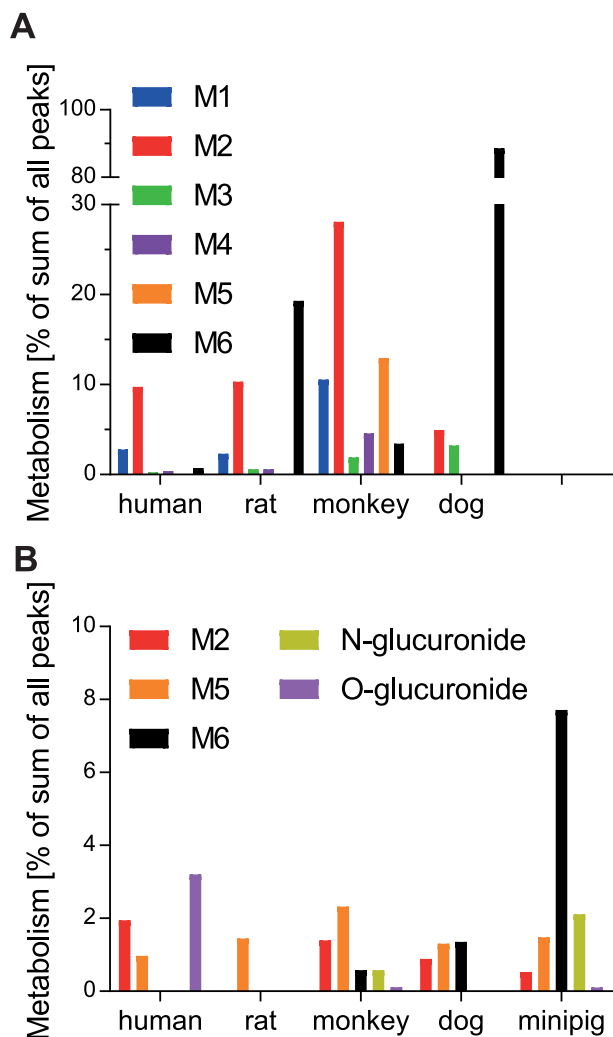


**Fig. 4.** A) Proposed Phase I metabolism of SUL-138. M1–5 metabolites were identified in liver microsomes from humans (HLM), Cynomolgus monkeys (MnkyLM), Beagle dogs (DLM) and Sprague-Dawley rats (RLM) as well as in hepatocytes from humans (Hhep), monkeys (MNKhep), dogs (Dhep), rats (Rhep) and Gottingen minipig (MPhep) using LC-MS/MS. B) Identified products of Phase I and II metabolism in hepatocytes.

oxidation of M2 in human microsomes yielded the less abundant M3 ( $t_R = 3.63$  min). This metabolite was formed either by N-oxidation (M3A) or hydroxylation at the piperazinyli moiety (M3B, Fig. 4A). Direct oxidation of piperazinyli moiety on SUL-138 in human microsomes and

hepatocytes led to the formation of M4 ( $t_R = 3.80$  min) more abundantly in human hepatocytes than microsomes (Fig. 4A, Fig. 5). N-oxidation of the tertiary amine of SUL-138 produced M5 ( $t_R = 4.53$  min) in human liver microsomes but not hepatocytes (Fig. 4A, Fig. 5). Moreover, there





**Fig. 5.** Quantification of metabolites of SUL-138. A) Peak areas of metabolites detected by LC-MS/MS in human, monkey, dog, rat liver microsomes and B) human, monkey, dog, rat and minipig hepatocytes (B).

was clear indication that SUL-138 forms a glucuronide conjugate in human hepatocytes, in fact two distinct glucuronides were formed (Fig. 4B, Fig. 5B). Given that UDP-glucuronosyl-transferase can catalyze both O- and N-glucuronidation, we propose two O-glucuronides, namely on the ethanolamine portion of the compound and the 6-hydroxy site, the N-glucuronide being on the piperazine ring. The N-glucuronide was predominantly produced by monkey and minipig hepatocytes, and the O-glucuronide by human hepatocytes (Fig. 5B).

Theoretically, further oxidation at the piperazinyl moiety of M3A and/or M3B may lead to desaturation and N-dealkylation, as depicted in Fig. 4. Also, the metabolite M4 may be further desaturated and N-dealkylated (Fig. 4A) and an additional N-dealkylation of M5 may result in the formation of SUL-151, the (S)-enantiomer of SUL-121 (Fig. 4A). However, these reaction products were absent in all MS analyses.

#### 3.4.4. *Cynomolgus monkey*

Similar to human microsomes, the *Cynomolgus monkey* liver microsomes metabolized SUL-138 largely to M1 and M2 (Fig. 5A), and M2 was also produced by both human and monkey hepatocytes (Fig. 5B). The metabolite M4 was found in higher amounts in monkey compared to human hepatocytes (tR = 3.80 min). Moreover, monkey microsomes produced M4m via oxidation, a later eluting (tR = 4.42 min) metabolite with reportedly the same structure and molecular weight as M4 (Fig. 4A, Fig. 5A). Relatively small quantities of M5 were detected in monkey

microsomes and hepatocytes (Fig. 4, Fig. 5). Monkey hepatocytes also demonstrated phase II metabolism, both N- and O-glucuronide conjugates of SUL-138 were measured (Fig. 4B, Fig. 5).

#### 3.4.5. *Beagle dog*

In dog microsomes, the M2 metabolite was found in slightly lower quantities compared to human microsomes, possibly due to a conversion of M2 to M3 (Fig. 4A, Fig. 5A). This conversion along with higher quantities of M5 suggest a rapid phase I metabolism of SUL-138 by the dog liver. Indeed, this is supported by higher levels of M2, M4 and M5 detected in dog than in human hepatocytes (Fig. 5). No phase II products were detected in dog hepatocytes (Fig. 5B).

#### 3.4.6. *Sprague-Dawley rat*

M2 and M5 were measured in large quantities in rat liver microsomes, whereas the only rat hepatocyte metabolite detected was M4. Similar to dog hepatocytes, no phase II metabolites were found (Fig. 5).

#### 3.4.7. *Gottingen minipig*

Finally, the metabolism of SUL-138 was investigated in Gottingen minipig hepatocytes. The most abundant phase I metabolite was M5, but also amounts of M2 and M4 were found (Fig. 4, Fig. 5). Minipig hepatocytes also produced the highest quantities of N-glucuronide conjugate of all hepatocyte species, while the amount of O-glucuronide was similar to monkey hepatocytes (Fig. 5B).

The molecular structure of SUL-138 offers several sites for oxidation during phase I metabolism. Considering that M2 is the most abundant product of phase I metabolism in human microsomes and hepatocytes, the most important reaction for human metabolism seems to constitute the oxidative opening of the chromane scaffold and formation of a quinol (M2, Fig. 4A, Fig. 5).

### 3.5. *In silico toxicity*

Based on its efficacy and pharmacokinetics *in vitro*, SUL-138 and metabolites were further investigated *in silico* to predict safety using Toxtree (Patlewicz et al., 2008). To calibrate sensitivity, we included Trolox, piperazine and 1-(2-hydroxyethyl)-piperazine which are used in the synthesis of SUL compounds. According to the Cramer rule (Cramer et al., 1976) of absence of sulphonate or sulphamate groups in a drug molecule, SUL-138 and its metabolites were classified as Class III substances, without a strong initial presumption of safety. Genotoxic and nongenotoxic carcinogenicity was predicted negative for all compounds tested for *in silico* toxicity (Table 3). Moreover, no alerts were raised by Toxtree for *in vitro* mutagenicity assays (AMES test) in *Salmonella typhimurium* (Table 3). Finally, Toxtree raised one positive structural alert for Trolox as prediction for *in vivo* micronucleus assay (Table 3) due to the presence of 3-spaced hydrogen acceptors which can cause non-covalent binding to DNA.

### 3.6. *In vitro genetic toxicity*

To validate the *in silico* toxicity prediction, the genotoxicity of SUL-138 was assessed at 5–100  $\mu$ M. All concentrations were negative for mutagenicity in the Ames fluctuation test in *S. typhimurium* and cultures of *S. typhimurium* with rat liver metabolic activation system (S9). Moreover, SUL-138 and its primary metabolites tested negative in bacterial cytotoxicity assays in reverted *S. typhimurium* as well as negative for chromosome aberrations in the micronucleus test in CHO-K1 cells and CHO-K1 cells with S9.

### 3.7. *Binding and enzyme interaction screen*

We explored the binding specificity of SUL-138 for a wide range of receptors and enzymes. In radioactive ligand assays, SUL-138 did not compete for binding to G-protein coupled receptors (Supplemental

**Table 3**

In silico toxicity prediction for SUL-138 compounds, metabolites and synthesis substrates. \* applies for oral administration of the compound.

Compound	Toxicology by Cramer rules (Patlewicz et al., 2008; Cramer et al., 1976; Munro et al., 1996)	Carcinogenicity (R. Benigni et al., 2013; Benigni et al., 2007)	In vitro mutagenicity (AMES) (Benigni and Bossa, 2011; R. Benigni et al., 2013)	In vivo micronucleus assay (Benigni et al., 2010)
SUL-138	High (Class III)	Negative for genotoxic and nongenotoxic	No alerts for S. Typhimurium	At least one positive structural alert (Class I)
Oxidation product	High (Class III)	Negative for genotoxic and nongenotoxic	No alerts for S. Typhimurium	At least one positive structural alert (Class I)
Oxidation	High (Class III)	Negative for genotoxic and nongenotoxic	No alerts for S. Typhimurium	At least one positive structural alert (Class I)
Oxidation ring opening	High (Class III)	Negative for genotoxic and nongenotoxic	No alerts for S. Typhimurium	At least one positive structural alert (Class I)
Oxidation of opened metabolite	High (Class III)	Negative for genotoxic and nongenotoxic	No alerts for S. Typhimurium	At least one positive structural alert (Class I)
Trolox	High (Class III)	Negative for genotoxic and nongenotoxic	No alerts for S. Typhimurium	At least one positive structural alert (Class I)

Figure 1A), ion channels, nuclear receptors or other receptors (Supplemental Figure 1B), or enzymes and transporters (Supplemental Figure 1C). Moreover, SUL-138 was screened against a set of enzymes, of which only 5-lipoxygenase (5-LO) appeared to be partly inhibited (Supplemental Figure 1C). The 5-LO activity assay performed to obtain these data used the fluorescent probe H<sub>2</sub>-DCFDA. However, given the nature of H<sub>2</sub>-DCFDA, SUL-138 is expected to react directly with the probe and decrease fluorescence, resulting in a false positive test result. To test this, 5-LO activity was measured by spectrophotometry by quantifying conjugated diene formation from arachidonic acid. Conjugate diene production in the presence of vehicle was  $106 \pm 12.9 \text{ nM s}^{-1}$ , which was unaffected by SUL-138 at concentrations used in the fluorescent assay (Supplemental Figure 2A, B). Based on these results we conclude that SUL-138 is not an inhibitor of 5-LO activity.

### 3.8. In vitro cardiovascular safety

Before initiating animal studies, SUL-138 and other compounds were investigated for cardiovascular safety. None of the tested compounds demonstrated *in vitro* inhibition of potassium current mediated by hERG ( $IC_{50} > 10 \mu\text{M}$ ).

**Table 4**

Pharmacokinetic characterization of SUL compounds tested in animals. Values are presented as mean  $\pm$  SEM.  $t_{\text{max}}$ , time to reach maximum plasma concentration;  $C_{\text{max}}$ , maximum plasma concentration,  $AUC_{\text{last}}$ , area under the plasma concentration curve from first to last measurement;  $AUC_{\infty}$ , AUC from first measurement to infinity;  $AUC_{\text{extrap}}$ , AUC extrapolated from time t to infinity as% of AUC;  $V_z$ , apparent volume of distribution during terminal phase; apparent total body clearance,  $t_{1/2}$ ; terminal half-life.

Compound	Model	n	Dose [mg/kg]	Route	$t_{\text{max}}$ [h]	$C_{\text{max}}$ [mg/L]	$AUC_{\text{last}}$ [h $\times$ mg/L]	$AUC_{\infty}$ [h $\times$ mg/L]	$AUC_{\text{extrap}}$ [%]	$V_z$ [L/kg]	CL [L/h]	$t_{1/2}$ [h]
SUL-150	mouse	2	10.0	iv bolus	0.16 $\pm$ 0.00	4.59 $\pm$ 0.05	3.70 $\pm$ 0.46	3.70 $\pm$ 0.46	0.11 $\pm$ 0.01	0.31 $\pm$ 0.05	0.08 $\pm$ 0.01	2.66 $\pm$ 0.01
SUL-151	mouse	3	10.0	iv bolus	0.16 $\pm$ 0.00	3.40 $\pm$ 0.16	2.57 $\pm$ 0.12	2.58 $\pm$ 0.12	0.17 $\pm$ 0.01	0.48 $\pm$ 0.06	0.11 $\pm$ 0.01	3.12 $\pm$ 0.11
SUL-109	mouse	2	10.0	iv bolus	0.16 $\pm$ 0.00	5.27 $\pm$ 0.68	3.87 $\pm$ 0.19	3.87 $\pm$ 0.19	0.10 $\pm$ 0.01	0.27 $\pm$ 0.03	0.07 $\pm$ 0.00	2.55 $\pm$ 0.07
	mouse	4	30.0	oral gavage	2.13 $\pm$ 1.63	0.39 $\pm$ 0.04	2.59 $\pm$ 0.86	2.16 $\pm$ 0.75	20.25 $\pm$ 15.03	4.39 $\pm$ 0.97	0.60 $\pm$ 0.31	6.97 $\pm$ 2.53
SUL-138	rat	6	0.4	iv bolus	0.17 $\pm$ 0.00	0.31 $\pm$ 0.05	0.28 $\pm$ 0.02	0.29 $\pm$ 0.02	4.90 $\pm$ 1.92	5.26 $\pm$ 1.68	0.86 $\pm$ 0.07	4.37 $\pm$ 1.44
	rat	5	2.0	iv bolus	0.17 $\pm$ 0.00	1.53 $\pm$ 0.12	1.32 $\pm$ 0.24	1.60 $\pm$ 0.33	18.33 $\pm$ 7.01	4.26 $\pm$ 2.05	0.95 $\pm$ 0.31	6.67 $\pm$ 3.89
	rat	5	10.0	iv bolus	0.17 $\pm$ 0.00	7.83 $\pm$ 0.64	7.52 $\pm$ 0.97	7.64 $\pm$ 0.97	1.79 $\pm$ 0.90	4.45 $\pm$ 1.57	0.71 $\pm$ 0.07	4.00 $\pm$ 1.05
	rat	6	10.0	oral gavage	0.17 $\pm$ 0.00	3.45 $\pm$ 0.52	4.97 $\pm$ 0.62	5.06 $\pm$ 0.60	2.51 $\pm$ 1.07	12.08 $\pm$ 3.58	1.26 $\pm$ 0.16	6.10 $\pm$ 0.95
SUL-138	rat	3	0.4	bolus-infusion	0.83 $\pm$ 0.58	0.05 $\pm$ 0.00	0.11 $\pm$ 0.01	0.11 $\pm$ 0.01	1.04 $\pm$ 0.56	8.15 $\pm$ 1.85	1.18 $\pm$ 0.11	4.68 $\pm$ 0.68
	rat	3	1.3	bolus-infusion	0.58 $\pm$ 0.22	0.11 $\pm$ 0.00	0.29 $\pm$ 0.01	0.30 $\pm$ 0.02	2.99 $\pm$ 1.36	15.73 $\pm$ 2.19	1.55 $\pm$ 0.07	7.12 $\pm$ 1.28
	rat	3	3.9	bolus-infusion	0.75 $\pm$ 0.25	0.49 $\pm$ 0.04	1.02 $\pm$ 0.10	1.05 $\pm$ 0.11	2.50 $\pm$ 0.92	12.00 $\pm$ 2.76	1.28 $\pm$ 0.17	6.89 $\pm$ 2.21

### 3.9. In vivo pharmacokinetics

Based on the *in vitro* and *in silico* compound library screening, SUL-138 was selected as the lead candidate for pre-clinical development in animals. However, before proceeding, an estimation of cardiovascular and respiratory safety of SUL-138 was made by inference from structural analogy with 6-chromanols which were already tested in animals. Since the therapeutic effects of the racemates SUL-121 and SUL-109 for different indications were already proven by previous studies (Lambooy et al., 2017; Han et al., 2016), they were tested in mice before SUL-138 emerged as a lead candidate for the prevention of AKI. This step was in accordance with the reduction and refinement principles of the Dutch laboratory animal practice guidelines.

#### 3.9.1. Studies in mice

The enantiomers of SUL-121, SUL-150 and SUL-151 and the racemic mixture SUL-109 were administered as a single intravenous bolus (10 mg/kg) in mice and blood plasma was sampled for 24 h. Terminal half-life for intravenous bolus administration (10 mg/kg) amounted  $2.66 \pm 0.01$  h for SUL-150,  $3.12 \pm 0.11$  h for SUL-151 and  $2.55 \pm 0.07$  h for SUL-109. The half-life for oral gavage administration of 30 mg/kg SUL-

109 was  $6.67 \pm 2.19$  h. In addition, SUL-109 was administered orally by gavage (30 mg/kg) and tracked in plasma for 24 h. Pharmacokinetic parameters were calculated using non-compartmental analysis (Table 4) and an oral bioavailability of SUL-109 in mice was estimated at  $F = 0.23$ .

### 3.9.2. Studies in rats

To obtain an initial plasma profile, the compound SUL-138 was administered to rats as a single intravenous bolus (0.4 mg/kg, 2.0 mg/kg and 10 mg/kg) and orally (10 mg/kg) and six blood samples were collected over the course of 24 h. The non-compartmental pharmacokinetic parameter estimates are shown in Table 4. Intravenous exposure of SUL-138 was proportional to dose (Fig. 6A) with terminal half-lives of SUL-138 amounting  $4.37 \pm 1.44$  h (0.4 mg/kg dose),  $6.67 \pm 3.89$  h (2.0 mg/kg dose) and  $4.00 \pm 1.05$  h (10 mg/kg dose) and an oral bioavailability  $F = 0.67$  (Table 4).

To investigate drug availability in target tissue, a separate study was performed. Considering proportional drug-exposure and the volume of distribution obtained from the first study in rats, we calculated bolus-priming doses and 2-h intravenous infusion rates which would achieve steady-state. After a bolus injection of 0.1, 0.3 and 0.9 mg/kg, animals were infused for 2 h at 0.15, 0.5 and 1.5 mg/kg/hr to a total dose of 0.4 mg/kg, 1.3 mg/kg, and 3.9 mg/kg of SUL-138, respectively. Blood plasma (11 time points) and kidney samples (5 time points) were collected at the end of infusion and until 24 h after. Results from non-compartmental pharmacokinetic analysis are shown in Table 4. Similar to our initial study in rats, we observed a proportional increase in  $AUC_{last}$  and  $C_{ss}$  to the infused amount of drug (Fig. 6B, C) and consistent clearance (Table 4). Calculated terminal half-lives of bolus-primed infusions of SUL-138 were  $4.68 \pm 0.68$  h (0.4 mg/kg dose),  $7.12 \pm 1.28$  h (1.3 mg/kg dose) and  $6.89 \pm 2.21$  h (3.9 mg/kg dose) (Table 4). More importantly, levels of SUL-138 were measured in the kidney (Fig. 7). After ceasing infusion, a two-phase elimination profile was observed in both plasma and kidney, suggesting multi-compartmental pharmacokinetics (Fig. 7). Moreover, the AUC ratios between kidney and plasma for all three dosing regimens were comparable ( $1.86 \pm 0.17$  mL/g, Supplemental Figure 3).

Since SUL-138 was developed as prophylactic treatment for kidney damage due to I/R during surgery, the effects of I/R on drug elimination were assessed in an additional study with rats undergoing I/R after pre-treatment with bolus-primed, continuous i.v. infusions of three different dosing regimens of SUL-138 (0.4 mg/kg, 1.3 mg/kg and 3.9 mg/kg). The resulting clearances did not differ from those observed in the previous rat studies and amounted  $1.10 \pm 0.07$  L/h,  $1.11 \pm 0.06$  L/h and  $0.92 \pm 0.06$  L/h, respectively (one-way ANOVA  $p = 0.08$ ).

In summary, the *in vivo* disposition profile of SUL-138 was characterized by distribution to the kidney, dose-exposure relationship that facilitated the calculation of doses for bolus-primed infusions, and a two-phase elimination with a suitable half-life that was unaffected by renal I/R.

### 3.10. *In vivo* cardiovascular and respiratory safety

The racemate SUL-121 was previously found to transiently affect the heart rate and mean arterial blood pressure (MAP) in rats subjected to a low 0.135 mg/kg/h i.v. infusion (Vogelaar et al., 2018). In a separate experiment, the (*R*)-enantiomer SUL-150 acutely decreased heart rate in mice from 450 to 300 bpm, which was rapidly restored with a normalization half-time of 6 s. This effect was not observed in mice after administering the (*S*)-enantiomer SUL-151. The racemate SUL-109 caused a decrease in heart rate in mice after 10 mg/kg intravenous bolus dose. Under the assumptions that a) the enantiomers of SUL-109 are metabolic precursors of the enantiomers of SUL-121, and b) the stereochemistry of SUL-109 also plays a role in mediating heart rate or MAP, we predicted that the (*S*)-enantiomer SUL-138 will not have cardiovascular effects.

To verify cardiovascular safety of SUL-138 in the setting of AKI,

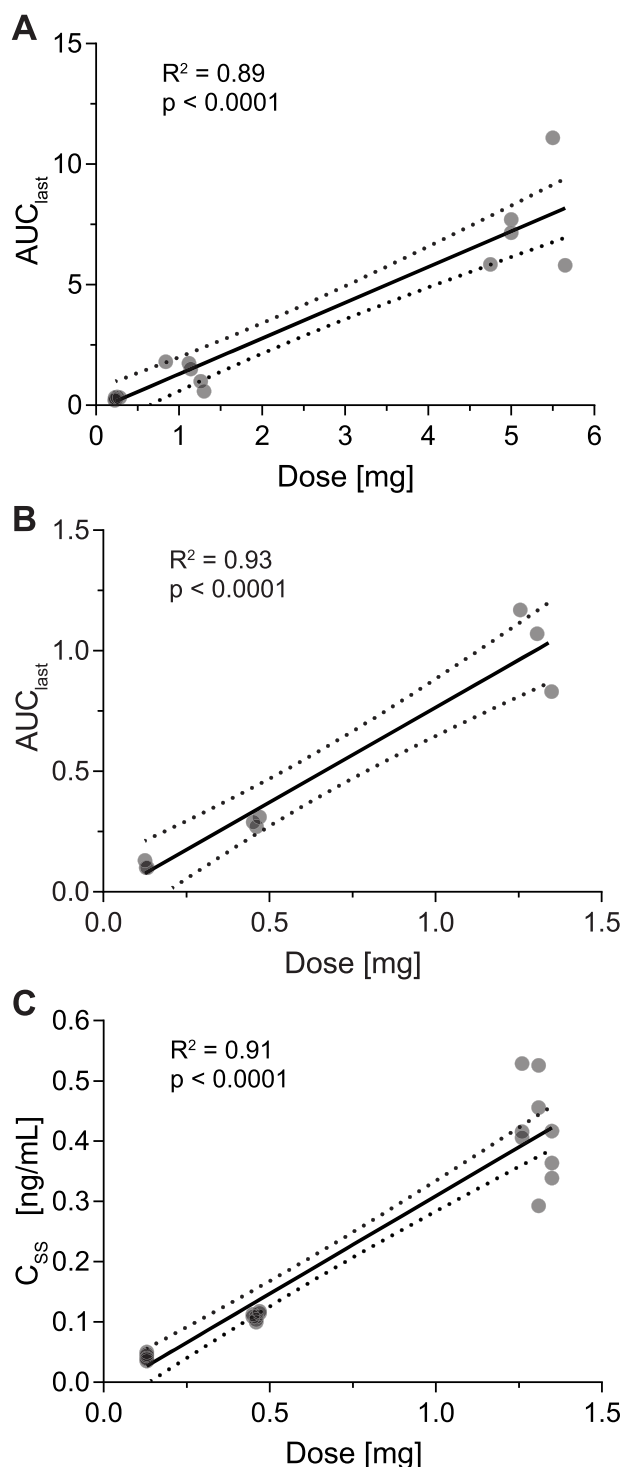
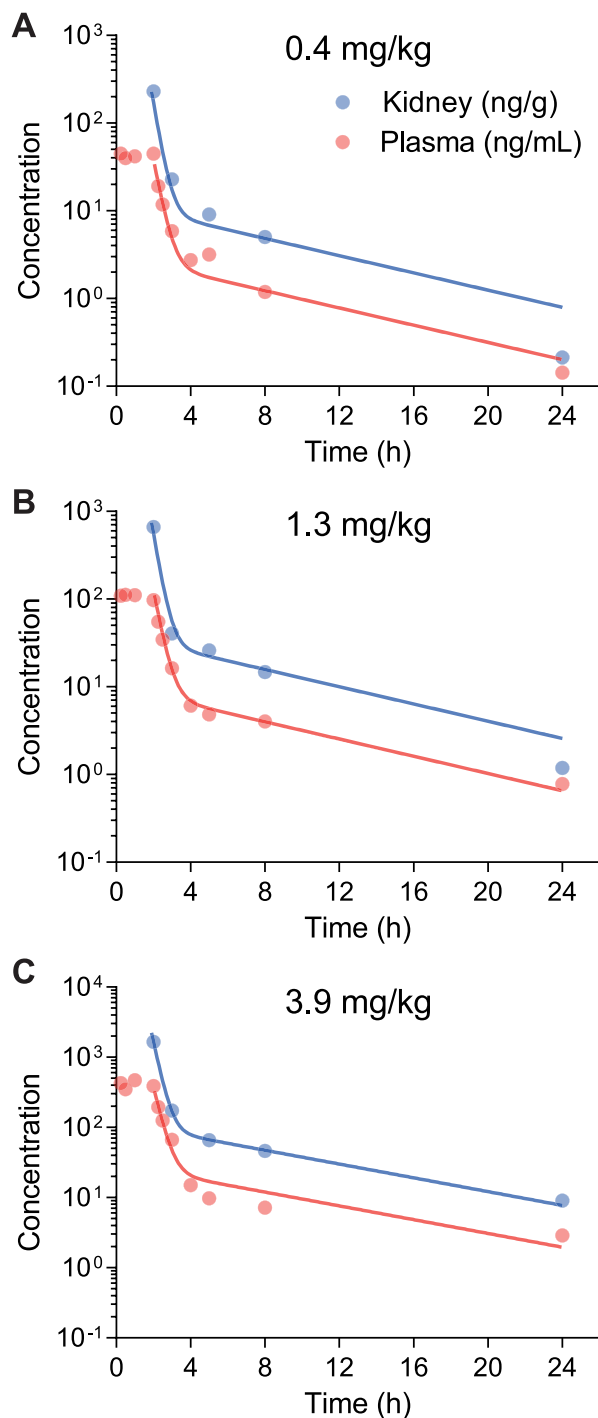


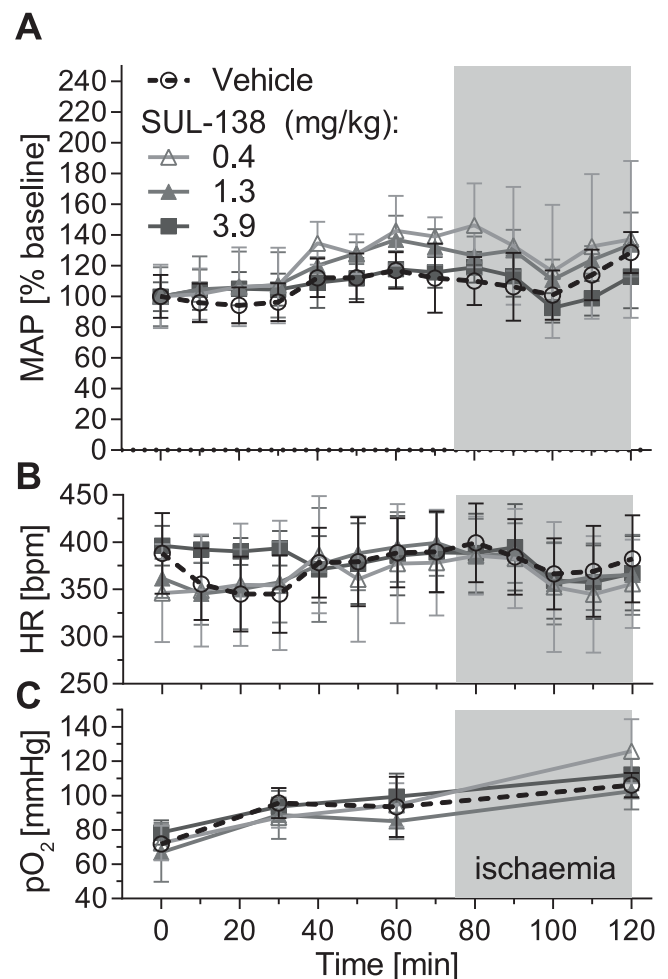
Fig. 6. Exposure represented by  $AUC_{last}$  and  $C_{ss}$  is proportional to dose during treatment of rats with SUL-138. Data from two separate studies in rats, in which A) animals were treated with 0.4 mg/kg, 2.0 mg/kg and 10 mg/kg intravenous bolus of SUL-138 and B) and C) bolus-primed infusion of 0.4 mg/kg, 1.3 mg/kg and 3.9 mg/kg SUL-138.

hemodynamic parameters were monitored during sham or I/R. Rats were sham operated or subjected to 45 min I/R by bilateral renal artery clamping and pre-treated with an initial i.v. bolus followed by continuous infusion of SUL-138 or vehicle throughout the clamping. In this experiment, five groups of animals were employed: a sham group which did not receive SUL-138 or renal clamp, and I/R groups treated with vehicle or 0.4 mg/kg, 1.3 mg/kg, and 3.9 mg/kg of SUL-138. During the



**Fig. 7.** Pharmacokinetic profile of bolus-primed infusion of SUL-138 in rats. Total amounts of SUL-138 administered were 0.4 mg/kg, 1.3 mg/kg and 3.9 mg/kg. Points represent concentrations of SUL-138 that were measured in plasma and kidney samples ( $n = 3$  plasma,  $n = 1-2$  kidney, per dosing regimen). Lines represent biphasic concentration profiles which were modeled per compartment (kidney or plasma) and in which dose was used as covariate. Overall, the two models hold well in all dosing regimens.

experiment, all I/R groups experienced a drop in MAP after clamping followed by a rebound halfway through renal ischemia (Fig. 8A, Supplemental Figure 4A). SUL-138 did not affect MAP in any dosing regimen during pre-treatment, nor during I/R (Fig. 8A). Moreover, heart rate was the same in all treatment groups throughout the experiment (Fig. 8B, Supplemental Figure 4B). Finally,  $pO_2$  rose from  $\sim 72$  mmHg 75 min prior to I/R to  $\sim 110$  mmHg at the end of renal artery clamping



**Fig. 8.** Cardiovascular and respiratory safety. A) mean arterial pressure in IR animals treated with vehicle or different doses of SUL-138. B) Heart rate in IR animals treated with vehicle or SUL-138. C) partial oxygen pressure in animals undergoing IR treated with vehicle or SUL-138.  $N = 6$  rats per group, data is shown as means  $\pm$ SD.

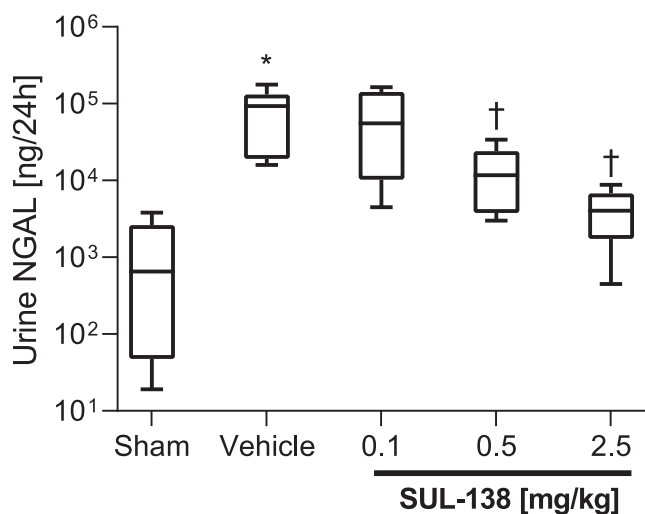
(Fig. 8C). There were no differences in  $pO_2$  between the sham and I/R-procedure groups treated with vehicle (Supplemental Figure 4C) or groups treated with SUL-138 (Fig. 8C). In summary, the three dosing regimens of SUL-138 did not alter MAP, heart rate or  $pO_2$ , therefore establishing the no-observed-adverse-effect level (NOAEL) for cardiovascular and respiratory effects of SUL-138 in rats to at least 3.9 mg/kg.

### 3.11. In vivo efficacy

Given that SUL-138 had a promising safety profile *in vitro* and was well tolerated *in vivo*, we next evaluated the efficacy in prophylaxis of AKI *in vivo*. Rats were subjected to 45 min I/R by bilateral renal artery clamping and pre-treated with a slow i.v. bolus of SUL-138 at 0.1, 0.5 and 2.5 mg/kg or vehicle throughout the clamping. Vehicle treated I/R animals displayed a decrease in 24 h urine production when compared to sham animals, to an extent where urine volume almost equaled water intake (Table 5, sham vs vehicle), which was normalized SUL-138 (Table 5). I/R also induced early renal dysfunction as evidenced by an increase in urinary creatinine and urea in the vehicle group compared to sham (Table 5). SUL-138 dose-dependently normalized these markers (Table 5). I/R induced a 70-fold increase in urinary NGAL amounting  $8.59 \times 10^4$  ng/24 h in the vehicle group compared to sham amounting  $1.24 \times 10^3$  ng/24 h (Fig. 9,  $p < 0.001$ , Dunnett's multiple comparison ANOVA). SUL-138 dose-dependently decreased NGAL (Fig. 9), with only

**Table 5**Data is expressed as means  $\pm$  SEM and were analysed by Fisher LSD test.

	Sham	Ischemia-Reperfusion			
		Vehicle	SUL-138 [mg/kg]		
			0.1	0.5	2.5
Urine volume [mL]	25.9 $\pm$ 11.3	16.9 $\pm$ 5.9	22.1 $\pm$ 6.9	22.2 $\pm$ 10.2	20.1 $\pm$ 10.3
Urine volume [% intake]	33.9	97.2	59.0	59.3	52.3
Urine pH	8.0 $\pm$ 0	7.0 $\pm$ 0.6 <sup>a</sup>	7.4 $\pm$ 0.7	7.5 $\pm$ 0.5	7.3 $\pm$ 0.5
Creatinine [mmol/L]	3.7 $\pm$ 0.2	8.0 $\pm$ 3.3 <sup>a</sup>	4.1 $\pm$ 2.0 <sup>b</sup>	5.2 $\pm$ 3.0 <sup>b</sup>	3.3 $\pm$ 1.4 <sup>b</sup>
Urea [mmol/L]	260.1 $\pm$ 63.9	581.8 $\pm$ 338.5 <sup>a</sup>	357.4 $\pm$ 187.5 <sup>b</sup>	347 $\pm$ 220.2 <sup>b</sup>	378.4 $\pm$ 78.7 <sup>b</sup>
Na <sup>2+</sup>	29.3 $\pm$ 19	39.8 $\pm$ 25.8	24.6 $\pm$ 6.7	33.4 $\pm$ 17.0	24.4 $\pm$ 9.8
K <sup>+</sup>	61.7 $\pm$ 28.1	145.3 $\pm$ 80.2 <sup>a</sup>	98.5 $\pm$ 3.9	87.5 $\pm$ 18.8 <sup>b</sup>	79.3 $\pm$ 31.7 <sup>b</sup>
Ca <sup>2+</sup>	0.7 $\pm$ 0.4	0.9 $\pm$ 0.5	0.6 $\pm$ 0.2	1.0 $\pm$ 0.3	0.5 $\pm$ 0.2
Mg <sup>2+</sup>	2.8 $\pm$ 0.4	6.1 $\pm$ 1.8 <sup>a</sup>	4.4 $\pm$ 1.9	5.9 $\pm$ 2.8	4.7 $\pm$ 1.0
PO <sub>4</sub> <sup>-3</sup>	165.6 $\pm$ 9	23.0 $\pm$ 5.4	15.7 $\pm$ 9.4	16.6 $\pm$ 12.5	12.6 $\pm$ 6.2 <sup>b</sup>

<sup>a</sup> p < 0.05 versus control.<sup>b</sup> p < 0.05 versus vehicle.**Fig. 9.** Total urine NGAL in urine collected over a period of 24 h. Data is shown as means (line), min-max box-and-whiskers and their individual data points. \*p < 0.05 versus sham, †p < 0.05 versus vehicle.

a minimal NGAL increase observed in I/R rats treated with the highest dose (2.5 mg/kg:  $4.21 \times 10^3$  ng/24 h). Thus, prophylactic treatment with SUL-138 prevented renal dysfunction in rats with I/R-induced AKI. No adverse effects of SUL-138 were observed upon macroscopic examination of the organs.

#### 4. Discussion

A compound library of 63 6-chromanols was developed with the aim to provide novel compounds for the protection from AKI (Van Der Graaf et al., 2014). We screened this library for pre-clinical safety and potency in protection of cells from cooling. The library was filtered using the Lipinski rule of 5<sup>20</sup> obtaining a subset of 15 druggable candidates, with too high or too low partition coefficients being the most common reasons for exclusion. Importantly, the 6-chromanols possessed on average a 1700-fold higher *In vitro* potency to protect HEK293 cells from hypothermia-induced cell death than Trolox. This difference cannot be attributed to basic pharmacological parameters such as molecular weight, TPSA or ClogP since they are closely similar for Trolox and

6-chromanols. Instead, the difference in efficacy is arguably caused by specific mitochondrial action that was demonstrated to be profound by SUL compounds, but not in Trolox (Hajmoussa et al., 2017). Notably, we have limited our *in vitro* experiments to a H/R model as opposed to a more common I/R model based on hypoxia/reoxygenation. In our experience, *in vitro* I/R was unable to consistently reproduce mitochondrial dysfunction, while H/R has successfully predicted improvements in kidney function due to mitochondrial dysfunction (Vogelaar et al., 2018).

The three candidates with the highest potency were SUL-121, SUL-132 and SUL-138. In addition, these compounds demonstrated favorable molecular weight, topological polar surface area and partition coefficient. It should be noted that in these studies SUL-121 was included as a racemic mixture and the enantiomers SUL-150 (*R*) and SUL-151 (*S*) were not screened individually. Conversely, the enantiomers SUL-132 (*R*) and SUL-138 (*S*) were assessed individually and their racemate SUL-109 was not included in *in vitro* studies.

Next, the pharmacokinetic properties of SUL compounds were assessed *in vitro*. As expected, the fraction of compound bound to plasma protein correlated with theoretical partition coefficient values (ClogP). Compounds SUL-121 and SUL-138 ranked average within the library for both parameters. Liver enzyme inhibition was low for the three lead candidates, suggesting low hepatic breakdown and absence of first-pass effects. Interestingly, the half-lives of SUL-121 and SUL-138 were more than doubled in human compared to rat liver microsomes while the  $t_{1/2}$  of SUL-132 did not differ between species. Taken together, *in vitro* pharmacokinetics suggested favorable properties of the three lead candidates providing the best prospects to reach therapeutic plasma and tissue levels.

In addition to the high efficacy of SUL-109 in the protection of HEK293 cells from cooling in our study, the (*S*)-enantiomer SUL-138 displayed favorable *in vitro* metabolism. Incubation of SUL-138 with microsomes revealed that rat phase I metabolism most closely resembled human phase I metabolism. The observed N-dealkylation is common for 6-chromanols, including tocopherols (Schmölz, 2016), and introduces the redox-active quinol/quinone system to the molecule (Schmölz, 2016). Also, opening of the chromane scaffold and formation of a quinol introduces a hydroxyl group to the molecule which may further be conjugated in phase II metabolism to facilitate excretion. However, it should be noted that this metabolic conversion is not required for SUL compounds to exert their main protective effects, given that the underlying mechanisms of action were previously demonstrated to encompass an action on mitochondrial complexes I and IV (Hajmoussa et al., 2017). Nevertheless, the formation of a quinol/quinone system from SUL-138 may grant the primary human metabolite redox activity and preserve the efficacy of the compound. Incubation of SUL-138 with hepatocytes showed that the predominant phase II metabolite is an O-glucuronide. Collectively, both phase I and II metabolism provide SUL-138 with a highly favorable metabolic profile, with potential for preserved antioxidant properties and solubilization for excretion. Based on the reported data on microsomal and hepatocyte metabolism, we identify rats and mini-pigs as the preferred species for further non-clinical development.

SUL-138 also displayed a promising toxicology profile despite two *in silico* alerts as these were addressed in follow-up experiments. A Toxtree warning of lack of solubilization was disproved based on evidence of metabolic hydroxylation and O-glucuronidation, and the risk of non-covalent binding to DNA due to hydrogen acceptors was excluded by negative results from tests for chromosome aberrations in the CHO-K1 micronucleus and Ames mutagenicity.

Slow i.v. bolus administration and oral gavage of the compounds SUL-109 and SUL-121 (10 mg/kg) in mice was well tolerated. Since SUL-150 had previously cardiovascular effects (Nakladal et al., 2019), the hemodynamically inactive (*S*)-enantiomer SUL-138 belonging to the racemic mixture SUL-109<sup>14,17</sup> was selected for further development.

Furthermore, SUL-138 was without effect on any of the 71 binding

targets and 25 enzymes that were investigated. The single positive hit, 5-lipoxygenase (5-LO), was proven to constitute a false negative result due to the antioxidant interference of SUL-138 in the assay principle. Further, SUL-138 did not inhibit the hERG channel. Together, these findings predicted no *in vivo* toxicity of SUL-138.

We expected that SUL-138 would not have hemodynamic effects since its chiral configuration resembles the vaso-inactive (*S*)-enantiomer of SUL-151. No animal deaths occurred in our studies due to administration of SUL compounds and there were no abnormalities recorded upon visual inspection of major organs during termination. No adverse cardiovascular (MAP, HR) effects were recorded in a dedicated safety study in rats. The absence of changes in pO<sub>2</sub> and pCO<sub>2</sub> suggest a lack of respiratory effects. Together, these observations suggest that doses can be further escalated and that NOAEL for cardiovascular and respiratory events will likely exceed the doses tested.

Given that SUL-138 passed the requirements for non-toxicity *in silico*, *in vitro* and *in vivo*, as well as *in vitro* metabolism, the pharmacokinetics of SUL-138 were subsequently investigated *in vivo*. As SUL-138 is currently under development for the prevention of surgery-associated AKI, i.v. administration is preferred over the oral route. However, for future indications such as diabetic nephropathy (Lambooy et al., 2017) the possibility of oral administration was also explored in rodents.

Oral administration of SUL-138 (10 mg/kg) in rats reflected the half-life of its parent racemic mixture SUL-109 (30 mg/kg) in mice and both were in the range of 6–7 hrs. In addition, the bioavailability in rats far exceeded that of mice, suggesting that future oral dosing regimens should be addressed with interspecies allometric scaling. Intravenous administration of SUL-138 as well as loading bolus dose followed by continuous infusion in rats yielded half-life estimates between 4 and 7 h, suggesting a favorable excretion half-life. Ceasing the infusion of SUL-138 in rats was followed by bi-phasic excretion profiles in plasma and kidney. Together with a volume of distribution that was higher than the total volume of all compartments in rats (12 L/kg), this observation indicated that SUL-138 was also distributed to other compartments than plasma. In the future, we aim to investigate in further detail the specific compartments that are involved in the uptake of SUL-138.

Moreover, drug AUC was proportional to dose in rats receiving single i.v. bolus or bolus-primed infusions and calculated total clearance in rats was constant (1.2 L/h on average) across dosing regimens of SUL-138. Finally, an I/R model in anesthetized rats was employed to rule out potentially altered drug elimination due to renal ischaemia. Firstly, SUL-138 plasma levels were not increased upon clamping of the renal arteries. Secondly, kidney concentrations of SUL-138 followed the same trend as plasma concentrations in healthy animals. Lastly, clearance in I/R rats was similar in differently dosed bolus-primed infusions of SUL-138 (1.10±0.07 L/h for 0.4 mg/kg, 1.11±0.06 L/h for 1.3 mg/kg and 0.92±0.06 L/h for 3.9 mg/kg), and was not different from the clearance measured in rats without I/R. For these reasons, plasma concentrations were considered an adequate indicator for compound selection. The unaffected clearance in a surgically induced I/R model support that SUL-138 is a suitable candidate for the treatment of AKI.

Importantly, SUL-138 prevented AKI in rats undergoing I/R, a model reflecting renal ischemia during extensive operations. To test prevention of AKI during surgical ischemia, SUL-138 was deliberately administered prior to and throughout the ischemic period and stopped immediately after. SUL-138 protected against early kidney injury as evidenced by increased urine output and decreased urinary creatinine as well as urea, and normalized the kidney damage marker, NGAL, at 24 h.

Our approach to select a drug candidate reflects the successful application of a classical phenotypical forward screening as an alternative to target-based high-throughput drug discovery. Notably, the current workflow resulted in nearly 5% of our library (3/63) being identified as highly feasible candidates for pre-clinical studies, demonstrating that small-scale approaches which combine low-throughput screening with thorough *in vitro* and *in silico* analysis may yield a high hit rate, confirming the track record of phenotypical screening (Vincent

et al., 2020). For future studies, a similar but less efficacious compound from our library should be included in *in vivo* studies to enable us to establish a clear structure-activity relationship.

Taken together, we present new evidence from pre-clinical characterization of a small library of hibernation-derived 6-chromanols, as well as insight into their pharmacokinetic and toxicology profiles. During screening, the compound SUL-138 emerged as a lead with favorable potency, non-carcinogenicity, and non-mutagenicity *in vitro* and a metabolite with putative antioxidant properties. We also report evidence of efficacy against AKI in rats. Further, it was established that SUL-138 has favorable pharmacokinetic profiles at different dosing regimens and administration routes. Bolus-primed infusion proved to be an appropriate treatment regimen of surgically induced I/R, without a requirement for repeated dosing after the procedure.

#### CRedit authorship contribution statement

**PC Vogelaar:** Visualization, Formal analysis, Writing – original draft. **D Nakladal:** Visualization, Formal analysis, Writing – original draft. **DH Swart:** Data curation. **Ľ Tkáčiková:** Visualization. **S Tkáčiková:** Visualization. **AC van der Graaf:** Data curation. **RH Henning:** Data curation, Visualization, Formal analysis, Writing – review & editing. **G Krenning:** Data curation, Formal analysis, Writing – original draft, Writing – review & editing.

#### Declaration of Competing Interest

Swart is chief of operations, van der Graaf is a stockholder and the chief executive officer, Vogelaar is researcher and Krenning is the chief scientific officer at Sulfateq (Groningen, The Netherlands), a company that owns patents on SUL-138 and produces and markets this and similar compounds. Van der Graaf reports personal fees from Sulfateq during the conduct of the study and has a patent (WO2014098586 A1) pending. Henning chairs the Scientific Advisory Board of Sulfateq. B.V. with contracts being approved by and payments being made to the UMCG. Dr. Henning holds no stocks or stock-options.

#### Acknowledgements

The authors would like to thank Martin C. Houwertjes for his expertise and effort during animal experiments.

#### Supplementary materials

Supplementary material associated with this article can be found, in the online version, at doi:10.1016/j.ejps.2021.106033.

#### References

- Acharya, C., Hooker, A.C., Türkyilmaz, G.Y., Jönsson, S., Karlsson, M.O., 2016. A diagnostic tool for population models using non-compartmental analysis: the ncappc package for R. *Comput. Methods Programs Biomed.* 127, 83–93.
- Artursson, P., 1990. Epithelial transport of drugs in cell culture. I: a model for studying the passive diffusion of drugs over intestinal absorptive (Caco-2) cells. *J. Pharm. Sci.* 79, 476–482.
- Benet, L.Z., Hosey, C.M., Ursu, O., Oprea, T.I., 2016. BDDCS, the rule of 5 and drugability. *Adv. Drug Deliv. Rev.* 101, 89–98.
- Benigni, R., Bossa, C., 2011. Mechanisms of chemical carcinogenicity and mutagenicity: a review with implications for predictive toxicology. *Chem. Rev.* 111, 2507–2536.
- Benigni, R., Bossa, C., Netzeva, T., Rodomonte, A., Tsakovska, I., 2007. Mechanistic QSAR of aromatic amines: new models for discriminating between homocyclic mutagens and nonmutagens, and validation of models for carcinogens. *Environ. Mol. Mutagen.* 48, 754–771.
- Benigni, R., Bossa, C., Tcheremenskaia, O., 2013b. Nongenotoxic carcinogenicity of chemicals: mechanisms of action and early recognition through a new set of structural alerts. *Chem. Rev.* 113, 2940–2957.
- Benigni, R., Bossa, C., Tcheremenskaia, O., 2013a. *In vitro* cell transformation assays for an integrated, alternative assessment of carcinogenicity: a data-based analysis. *Mutagenesis* 28, 107–116.
- Benigni, R., Bossa, C., Worth, A., 2010. Structural analysis and predictive value of the rodent *in vivo* micronucleus assay results. *Mutagenesis* 25, 335–341.

- Buscher, B., et al., 2014. Bioanalysis for plasma protein binding studies in drug discovery and drug development: views and recommendations of the european bioanalysis forum. *Bioanalysis* 6, 673–682.
- Carden, D.L., Granger, D.N., 2000. Pathophysiology of ischaemia-reperfusion injury. *J. Pathol.* 190, 255–266.
- Collister, D., et al., 2017. Health care costs associated with aki. *Clin. J. Am. Soc. Nephrol.* 12, 1733–1743.
- Cramer, G.M., Ford, R.A., Hall, R.L., 1976. Estimation of toxic hazard—A decision tree approach. *Food Cosmet. Toxicol.* 16, 255–276.
- Cyprotex, 2021. Caco-2 permeability assay. Caco-2 Permeability Assay Prod. n.d. *Sheet*.
- Diaz, D., Scott, A., Carmichael, P., Shi, W., Costales, C., 2007. Evaluation of an automated *in vitro* micronucleus assay in CHO-K1 cells. *Mutat. Res. Toxicol. Environ. Mutagen.* 630, 1–13.
- Dugbartey, G.J., et al., 2014. P24 renal protection through cbs/h2s pathway in mammalian hibernation: a natural model of hypothermic organ preservation during cold ischemia and reperfusion. *Nitric Oxide* 39, S23.
- Dugbartey, G.J., et al., 2015. Dopamine treatment attenuates acute kidney injury in a rat model of deep hypothermia and rewarming – the role of renal H2S-producing enzymes. *Eur. J. Pharmacol.* 769, 225–233.
- Gao, Y., et al., 2015. Polydatin inhibits mitochondrial dysfunction in the renal tubular epithelial cells of a rat model of sepsis-induced acute kidney injury. *Anesth. Analg.* 121, 1251–1260.
- Hajmoussa, G., et al., 2017. The 6-chromanol derivate SUL-109 enables prolonged hypothermic storage of adipose tissue-derived stem cells. *Biomaterials* 119, 43–52.
- Han, B., et al., 2016. The novel compound sul-121 inhibits airway inflammation and hyperresponsiveness in experimental models of chronic obstructive pulmonary disease. *Sci. Rep.* 6, 26928.
- International Society of Nephrology.** n.d. AKI - Oby25. <https://www.theisn.org/Oby25#acute-kidney-injury-aki>.
- Kerr, M., Bedford, M., Matthews, B., O'Donoghue, D., 2014. The economic impact of acute kidney injury in england. *Nephrol. Dial. Transplant.* 29, 1362–1368.
- Kirchmair, J., et al., 2015. Predicting drug metabolism: experiment and/or computation? *Nat. Rev. Drug Discov.* 14, 387–404.
- Lambooy, S.P.H., et al., 2017. The novel compound sul-121 preserves endothelial function and inhibits progression of kidney damage in type 2 diabetes mellitus in mice. *Sci. Rep.* 7.
- Larregieu, C.A., Benet, L.Z., 2013. Drug discovery and regulatory considerations for improving *in silico* and *in vitro* predictions that use caco-2 as a surrogate for human intestinal permeability measurements. *AAPS J.* 15, 483–497.
- Levey, A.S., James, M.T., 2017. Acute kidney injury. *Ann. Intern. Med.* 167, ITC66.
- Lipinski, C.A., Lombardo, F., Dominy, B.W., Feeney, P.J., 1997. Experimental and computational approaches to estimate solubility and permeability in drug discovery and development settings. *Adv. Drug Deliv. Rev.* 23, 3–25.
- Maron, D.M., Ames, B.N., 1983. Revised methods for the salmonella mutagenicity test. *Mutat. Res.* 113, 173–215.
- Masferrer, J.L., et al., 2010. Pharmacology of PF-4191834, a novel, selective non-redox 5-Lipoxygenase inhibitor effective in inflammation and pain. *J. Pharmacol. Exp. Ther.* 334, 294–301.
- Mehta, R.L., et al., 2016. Recognition and management of acute kidney injury in the international society of nephrology Oby25 global snapshot: a multinational cross-sectional study. *Lancet North Am. Ed.* 387, 2017–2025.
- Morigi, M., et al., 2015. Sirtuin 3-dependent mitochondrial dynamic improvements protect against acute kidney injury. *J. Clin. Invest.* 125, 715–726.
- Munro, I.C., Ford, R.A., Kennepohl, E., Sprenger, J.G., 1996. Correlation of structural class with no-observed-effect levels: a proposal for establishing a threshold of concern. *Food Chem. Toxicol. Int. J. Publ. Br. Ind. Biol. Res. Assoc.* 34, 829–867.
- Nakladal, D., et al., 2019. The (R)-enantiomer of the 6-chromanol derivate SUL-121 improves renal graft perfusion via antagonism of the  $\alpha$ 1-adrenoceptor. *Sci. Rep.* 9.
- Patlewicz, G., Jeliakova, N., Safford, R.J., Worth, A.P., Aleksiev, B., 2008. An evaluation of the implementation of the cramer classification scheme in the toxtree software. *SAR QSAR Environ. Res.* 19, 495–524.
- R Core Team.** *R: a language and environment for statistical computing.* (R Foundation for Statistical Computing, 2019).
- Salzman, S.K., Lladós-Eckman, C., Beckman, A.L., 1986. Release and metabolism of dopamine and serotonin in the caudate nucleus during euthermia and hibernation. *Ann. N. Y. Acad. Sci.* 473, 267–283.
- Schmölz, L., 2016. Complexity of vitamin e metabolism. *World J. Biol. Chem.* 7, 14.
- Scott, J.W., Cort, W.M., Harley, H., Parrish, D.R., Saucy, G., 1974. 6-Hydroxychroman-2-carboxylic acids: novel antioxidants. *J. Am. Oil Chem. Soc.* 51, 200–203.
- Takano, M., et al., 1998. Interaction with P-glycoprotein and transport of erythromycin, midazolam and ketoconazole in caco-2 cells. *Eur. J. Pharmacol.* 358, 289–294.
- Talaei, F., et al., 2011. Reversible remodeling of lung tissue during hibernation in the syrian hamster. *J. Exp. Biol.* 214, 1276–1282.
- van Breeem, R.B., Li, Y., 2005. Caco-2 cell permeability assays to measure drug absorption. *Expert Opin. Drug Metab. Toxicol.* 1, 175–185.
- Van Der Graaf, A.C. van der, Heeres, A. & Paulus Gerardus Seerden, J. Compounds for protection of cells.** (2014).
- Veber, D.F., et al., 2002. Molecular properties that influence the oral bioavailability of drug candidates. *J. Med. Chem.* 45, 2615–2623.
- Vincent, F., et al., 2020. Hit triage and validation in phenotypic screening: considerations and strategies. *Cell Chem. Biol.* 27, 1332–1346.
- Vogelaar, P.C., et al., 2018. The 6-hydroxychromanol derivative SUL-109 ameliorates renal injury after deep hypothermia and rewarming in rats. *Nephrol. Dial. Transplant.* <https://doi.org/10.1093/ndt/gfy080>.**
- Wang, Y., Bellomo, R., 2017. Cardiac surgery-associated acute kidney injury: risk factors, pathophysiology and treatment. *Nat. Rev. Nephrol.* 13, 697–711.
- Zheng, Y., Yang, X., 2008. Absorption and transport of pachymic acid in the human intestinal cell line caco-2 monolayers. *Zhong Xi Yi Jie He Xue Bao* 6, 704–710.